

Model-free inference on extreme dependence via waiting times

James E. Johndrow
Duke University, Durham, NC USA
jj@stat.duke.edu

Robert L. Wolpert
Duke University, Durham, NC USA
wolpert@stat.duke.edu

March 2, 2022

Abstract

A variety of methods have been proposed for inference about extreme dependence for multivariate or spatially-indexed stochastic processes and time series. Most of these proceed by first transforming data to some specific extreme value marginal distribution, often the unit Fréchet, then fitting a family of max-stable processes to the transformed data and exploring dependence within the framework of that model. The marginal transformation, model selection, and model fitting are all possible sources of misspecification in this approach.

We propose an alternative model-free approach, based on the idea that substantial information on the strength of tail dependence and its temporal structure are encoded in the distribution of the waiting times between exceedances of high thresholds at different locations. We propose quantifying the strength of extremal dependence and assessing uncertainty by using statistics based on these waiting times. The method does not rely on any specific underlying model for the process, nor on asymptotic distribution theory. The method is illustrated by applications to climatological, financial, and electrophysiology data.

To put the proposed approach within the context of the existing literature, we construct a class of spacetime-indexed stochastic processes whose waiting time distributions are available in closed form by endowing the support points in de Haan’s spectral representation of max-stable processes with random birth times, velocities, and lifetimes, and applying Smith’s model to these processes. We show that waiting times in this model are stochastically decreasing in mean speed, and the sample mean of the waiting times obeys a central limit theorem with a uniform convergence rate under mild conditions. This indicates that our procedure can be implemented in this setting using standard t statistics and associated hypothesis tests.

Keywords: extreme value; max-stable process; peaks-over-thresholds; tail dependence; time series; waiting time.

1 Introduction

In applications where multivariate or spatial extremes are of interest, typically one has a collection of observations $w(\mathbf{x}, t) = (w(x_1, t), \dots, w(x_n, t))$ of a stochastic process $\{W(x, t)\}$ at a collection of locations x_1, \dots, x_n and times t_1, \dots, t_p in some study period $[T_0, T_0 + T]$. These observations could represent hourly precipitation, maximum daily wind speed, or, if we treat the spatial index set \mathcal{X} as a latent coordinate in an abstract attribute space, essentially any multivariate time series, such as daily stock prices. Inference often focuses on the strength of dependence at extreme quantiles for pairs of points x_1, x_2 .

Methods for estimation and inference often fit a particular parametric or semi-parametric model to data, then explore dependence within the context of this model. This is typically a model of a *max-stable process*. Prior to fitting, data have usually been transformed either by taking the maximum over time windows [38, 39], or keeping only data points where $w(\mathbf{x}, t)$ exceeds a threshold [11, 33], then transforming to a specific extreme value marginal distribution such as the unit Fréchet. The implicit assumption is that these “extreme” data are approximately realizations from the limiting max-stable process. In most cases the full likelihood under the model is intractable, so pseudo- or composite- likelihood methods are used.

Here we propose an alternative approach to inference about dependence in the extremes of a space-time indexed stochastic process, based on waiting times between threshold exceedances at pairs of spatial locations. Our procedure has two steps. We first compute an estimate of the distribution of waiting times between exceedances at pairs of spatial locations under the assumption that the process is independent at those points. We then estimate the distance between this “null” distribution and the empirical distribution of waiting times between exceedances at these two points in a suitable metric on probability measures. This estimate is our basic statistic quantifying dependence. We also propose methods for interval estimation and measures of significance. An advantage of this method over fitting a specified model directly to the data is that it does not rely on any assumptions about the underlying process and, in contrast to alternatives, is not based on any asymptotic approximation to the distribution of observed data. Unlike most alternatives, our approach does not require estimation or transformation of the marginals. Moreover, while the term “spatial locations” is a useful shorthand, we emphasize that the index set could be abstract and the locations unobserved, a point that we illustrate with financial applications. Our approach is also applicable to settings where max-stable modeling is not, such as multi-hazard risk management quantifying overall risk due to multiple sometimes-related hazards like hurricanes, earthquakes, volcanic eruptions, and tsunamis.

A significant portion of this paper is devoted to connecting our approach with existing methods for inference based on max-stable processes by constructing a particular model of a max-stable process in which the distribution of waiting times between exceedances is tractable. The model we construct is similar to that of [10] in that both are generalizations of [34] to space-time, and may be viewed as a special case of the models considered in [15]. Our aim is not to propose a new class of models for space-time indexed max-stable processes, but to construct a particular space-time indexed max-stable process in which we can easily study the distributions of waiting times. We show that waiting times in this model are stochastically decreasing in mean speed, and the sample mean of the waiting times obeys a central limit theorem. This indicates that in this setting, a form of our procedure can be implemented using standard t tests for the difference of means.

A *max-stable process* is defined by de Haan [12] to be a stochastic process $Y(x)$ on an index set \mathcal{X} with the property that, for all integers $n \in \mathbb{N}$,

$$Y(\cdot) \stackrel{\mathcal{D}}{=} \frac{1}{n} \bigvee_{i=1}^n Y_i(\cdot), \quad (1)$$

where $\{Y_i\}$ are iid copies of Y , where “ \vee ” denotes pointwise maximum, and where for two stochastic processes Y, Z the relation $Z(\cdot) \stackrel{\mathcal{D}}{=} Y(\cdot)$ means that all their finite-dimensional marginal distributions agree. Slightly different definitions appear elsewhere in the literature ([34; 5, §9.3; 31; 3, §8.2; 13, §9.2]). Some authors use the term “*simple* max-stable process” for those which satisfy (1) (and hence have Fréchet univariate marginal distributions with shape $\alpha = 1$) and extend the class of max-stable processes to those satisfying $Y(\cdot) \stackrel{\mathcal{D}}{=} [\bigvee_{i=1}^n Y_i(\cdot) - b_n(\cdot)]/a_n(\cdot)$ for suitable sequences of functions $a_n(\cdot) > 0$, $b_n(\cdot)$. In the spatial or spatio-temporal setting, one usually takes $\mathcal{X} = \mathbb{R}^d$ for some integer d .

There is a large literature on parametric models for max-stable processes. Two approaches are common for model building. The first uses the characterization of de Haan [12, 29]: a process $Z(x) := \sup_j u_j k(x, \xi_j)$ is max-stable if $k : \mathcal{X} \times \mathcal{X} \rightarrow \mathbb{R}_+$ is a nonnegative kernel satisfying $\int_{\mathcal{X}} k(x, \xi) m(d\xi) = 1$ and $\{u_j, \xi_j\}$ are points of a Poisson random Borel measure on $\mathbb{R}_+ \times \mathcal{X}$ with intensity measure proportional to $u^{-2} du m(d\xi)$ for some σ -finite Borel reference measure $m(dx)$ on \mathcal{X} . Smith [34] uses Gaussian kernels to construct a model in which the joint distribution of the process at two points is tractable (see also [7] and [32]). Theoretical characterizations of this model are found in Hüsler and Reiss [24]. Another example of this approach is the circular model of Coles and Walshaw [8].

The other main approach is based on the *spectral measure* [3, §8.2.3]. The most popular, and oldest, parametric model is the logistic model [18, 19]. Extensions of this model beyond the bivariate case were described by Tawn [39], Coles and Tawn [6]. Another example is the Dirichlet model of Coles and Tawn [6].

In either approach to max-stable modeling, data must be transformed prior to fitting, either by taking maxima over time windows or selecting only data that exceed a threshold. There are several

varieties of the latter, including: keeping observations at times t for which $\max_{i=1}^n w(x_i, t)$ exceeds a pre-specified threshold [30, 4]; fixing a specific component (say, x_1) and keeping observations at times t where $w(x_1, t)$ exceeds a threshold [22, 21, 9, 1]; and, keeping all observations at times t where some vector norm $\|w(\cdot, t)\|$ exceeds a threshold [6, 2]. In addition, one usually needs to estimate the margins; see Beirlant et al. [3, §9.3]. Fitting is usually performed using approximate likelihood methods.

A potential shortcoming of generic max-over-windows and peaks-over-thresholds approaches is that some temporal information is lost by the transformation process. More recently, a number of models explicitly incorporating a time dimension have been proposed. Huser and Davison [23] extend a model of Schlather [31] to the space-time setting. The model is constructed using the de Haan characterization, and thus the method essentially treats time as one component of the index set \mathcal{X} . Davis et al. [10] similarly extend the model of Smith [34] to the space-time setting, again treating one component of the index set \mathcal{X} as the time domain. One restrictive feature of these models is that the nature of dependence across space and time is the same. More recently, Embrechts et al. [15] proposes models in which temporal dependence structure can be different from spatial dependence structure when the process is Markovian in time.

2 Inference based on waiting times

2.1 Basic extremal dependence measure

Begin with a real-valued space-time indexed stochastic process

$$Y : \mathcal{X} \times \mathcal{T} \rightarrow \mathbb{R},$$

typically with spatial coordinate $x \in \mathcal{X} = \mathbb{R}^d$ and time coordinate $t \in \mathcal{T}$ with either continuous time $\mathcal{T} = \mathbb{R}_+$ or discrete time $\mathcal{T} = \mathbb{Z}_0 = \{0, 1, 2, \dots\}$ with the property that, for each fixed $x \in \mathcal{X}$, the process

$$t \mapsto Y(x, t)$$

is stationary and strong Markov. Our procedure does not require Markovianity, but it is more intuitive to motivate it in this context.

Fix a collection of (perhaps high) thresholds $y(x), x \in \mathcal{X}$, and consider the \mathcal{X} and $\mathcal{X} \times \mathcal{X}$ -indexed processes

$$V(x) := \inf\{t > 0 : Y(x, t) > y(x)\} \quad (2)$$

$$Z(x_1, x_2) := \inf\{t > V(x_1) : Y(x_2, t) > y(x_2)\} - V(x_1), \quad (3)$$

the waiting time until first exceedance of $y(x)$ at x , and the waiting time until the first exceedance of $y(x_2)$ at x_2 subsequent to an exceedance of $y(x_1)$ at x_1 . Let d be a semimetric on the space of probability measures and define

$$\gamma_d(x_1, x_2) := d(\mathcal{L}\{V(x_2)\}, \mathcal{L}\{Z(x_1, x_2)\}), \quad (4)$$

where $\mathcal{L}(Z)$ is the law of the random variable Z . If $Y(x_2, t) \perp\!\!\!\perp Y(x_1, t)$, then $\gamma_d(x_1, x_2) = 0$, whereas if there is strong dependence at high quantiles between $Y(x_1, \cdot)$ and $Y(x_2, \cdot)$, we would expect γ_d to be large. Thus, we propose to use estimates of $\gamma_d(x_1, x_2)$ based on samples of Y at pairs of locations x_1, x_2 to quantify the strength of dependence at high quantiles.

In many applications, it is likely that dependence at high quantiles of Y between locations x_1 and x_2 would result in the expectation of $Z(x_1, x_2)$ being smaller than the expectation of $V(x_2)$. In other words, extreme events at x_1 would tend to be followed soon thereafter by extreme events at x_2 . In this case, we can just choose the semimetric

$$d(\mu, \nu) = M(\mu, \nu) := \left| \int z(\mu - \nu)(dz) \right|, \quad (5)$$

the absolute difference in the expectations. We consider other, more general, choices of d later.

2.2 Procedure: estimation of $\mathcal{L}(V(x_2))$ and $\mathcal{L}(Z(x_1, x_2))$

Suppose initially that we observe $Y(x, t)$ at all times $t \geq 0$. Fix a site $x \in \mathcal{X}$ and collections of thresholds $\underline{y}(x) < \bar{y}(x)$ in the support of $Y(x, t)$, and set $\bar{s}_0 := 0$. Then for $j \in \mathbb{N}$, set

$$\begin{aligned} \underline{s}_j(x) &:= \inf\{t > \bar{s}_{j-1}(x) : Y(x, t) \leq \underline{y}(x)\}; \\ \bar{s}_j(x) &:= \inf\{t > \underline{s}_j(x) : Y(x, t) \geq \bar{y}(x)\}; \\ v_j(x) &:= (\bar{s}_j(x) - \underline{s}_j(x)). \end{aligned} \quad (6)$$

The $(\underline{s}_j(x), \bar{s}_j(x))$ are the times of the j th upcrossing of $(\underline{y}(x), \bar{y}(x))$ by $Y(x, \cdot)$ and $v_j(x)$ is its duration.

If instead of fixing $\underline{y}(x)$, we drew $\underline{y}(x)$ from the marginal distribution of $Y(x, t)$ – which by assumption of stationarity does not depend on t – then by the strong Markov property, $\{v_j(x)\}$ would be an iid sequence from exactly the distribution of interest, that of $V(x)$ in (2). We expect that $\{v_j(x)\}$ will have *approximately* the same distribution as $V(x)$ even with a fixed, appropriately chosen $\underline{y}(x)$, such as the median. In fact, if $Y(x, \cdot)$ were a finitely supported, discrete-time Markov process, it follows from Theorem 1 of [26] that the hitting time of the median is exactly the mixing time.

If we only observe $Y(x, t)$ on some interval $t \in [0, T]$ then only a finite number $J \geq 0$ of upcrossings will occur. In that case $\bar{s}_j(x)$ is infinite for $j > J$, so $J = \max\{j \geq 0 : \bar{s}_j(x) < \infty\}$. It is possible for J to be zero, i.e. to have no upcrossings before time T . In real applications the marginal distribution of Y will be estimated from the sample, and its quantiles used to determine thresholds, so this will not be a concern. Accordingly, we use

$$\hat{F}_{V(x)}(v) = J^{-1} \sum_{j=1}^J \mathbf{1}_{\{v_j(x) \leq v\}}, \quad (7)$$

the empirical distribution of $\{v_j(x)\}$, as an estimator of $\mathcal{L}(V(x))$.

Estimation of $\mathcal{L}(Z(x_1, x_2))$ is similar. Fix two locations $\{x_1, x_2\} \subset \mathcal{X}$ and thresholds $\underline{y}(x_1) < \bar{y}(x_1)$ and $\underline{y}(x_2) < \bar{y}(x_2)$ in the support of $Y(x, t)$. Define $\bar{\mathcal{S}}(x) = \{\bar{s}_j(x)\}$ as the set of all first exceedance times of $\bar{y}(x)$ at location x obtained using (6). Define $s_0^*(x_2) = 0$ and for $j \in \mathbb{N}$, set

$$\begin{aligned} s_j^*(x_1) &:= \inf\{t \in \bar{\mathcal{S}}(x_1) : t > s_{j-1}^*(x_2)\}; \\ s_j^*(x_2) &:= \inf\{t \in \bar{\mathcal{S}}(x_2) : t > s_j^*(x_1)\}; \\ z_j(x_1, x_2) &:= (s_j^*(x_2) - s_j^*(x_1)) \end{aligned} \quad (8)$$

This generates a sequence $\{z_j(x_1, x_2)\}$ of times to an exceedance at x_2 that follow one at x_1 . A similar algorithm will generate a sequence $\{z_j(x_2, x_1)\}$ of times to an exceedance at x_1 that follow one at x_2 . We use

$$\hat{F}_{Z(x_1, x_2)}(z) = J^{-1} \sum_{j=1}^J \mathbf{1}_{\{z_j(x_1, x_2) \leq z\}},$$

the analogue of (7), as an estimator of $\mathcal{L}\{Z(x_1, x_2)\}$. We then use

$$\hat{\gamma}_d(x_1, x_2) := \gamma_d(\hat{F}_{V(x_2)}, \hat{F}_{Z(x_1, x_2)})$$

as our estimator of $\gamma_d(x_1, x_2)$. In the case where d is the semimetric in (5), one can perform approximate classical tests of the hypothesis

$$H_0 : d = 0$$

using the Welch t statistic [40], and construct confidence intervals for the difference in means, with the one additional requirement that the central limit theorem holds the sample means $J^{-1} \sum_j v_j(x_2)$ and $J^{-1} \sum_j z_j(x_1, x_2)$.

In practice, it is often the case that $Y(x, t)$ is well-defined for all times $t \in \mathbb{R}_+$, but is observed only at an increasing sequence of times $\{t_i\}$. In this case, if we begin for some j with $Y(x, s_j(x))$ in

the stationary marginal distribution, and set $\bar{s}_j(x) = \inf\{t_i > \underline{s}_j(x) : Y(x, t_i) \geq \bar{y}\}$, then $v_j(x) := (\bar{s}_j(x) - \underline{s}_j(x))$ will always over-estimate the actual time-to-exceedance. In fact it could over-estimate by an arbitrarily large amount, since it is possible for $Y(x, t^*) \geq \bar{y}(x)$ for an unobserved time $t^* \in (\underline{s}_j(x), \bar{s}_j(x))$ that could be arbitrarily close to $\underline{s}_j(x)$. This problem is not peculiar to our setting, and arises any time a continuous-time process is sampled discretely. If the discrete sampling frequency is high enough for the gaps $(t_j - t_{j-1})$ to be small compared to the typical fluctuations of $Y(x, t)$, then the discrete approximation will be reasonably accurate. We will assume this is the case – were it not so, it would be a serious deficiency of the sampling design that would limit the usefulness of the data for most inference problems.

2.3 Alternative metrics d

In some cases, the assumption that the expectation of $Z(x_1, x_2)$ decreases as $Y(x_1, \cdot)$ and $Y(x_2, \cdot)$ become more highly dependent at high thresholds is not realistic. For example, neurons firing in one brain region may suppress neuronal activity in another brain region. As such, we consider some alternatives to the semimetric in (5).

A popular measure of discrepancy between empirical distributions is the Anderson-Darling two-sample statistic

$$\text{AD}(\hat{F}_V, \hat{F}_Z) = \frac{J_1 J_2}{J} \int_{-\infty}^{\infty} \frac{\{\hat{F}_V(z) - \hat{F}_Z(z)\}^2}{\hat{H}_J(x)\{1 - \hat{H}_J(x)\}} d\hat{H}_J(z),$$

where $\hat{H}_J(z)$ is the empirical distribution function of the combined sample, which consists of $J = J_1 + J_2$ observations. $\text{AD}(\cdot, \cdot)$ is also a proper distance between finite atomic measures.

Another distance we use is the Kolmogorov metric

$$\text{KS}(F_V, F_Z) = \sup_x |F(x) - G(x)| \quad (9)$$

for distribution functions F_V, F_Z . In finite samples this is estimated from the Kolmogorov-Smirnov statistic, which is just (9) evaluated for empirical distribution functions \hat{F}_V, \hat{F}_Z .

A third metric used here is a kernel metric studied in the machine learning literature [17, 16, 35, 36, 37, 17, 25] and defined as follows. Let $(\mathbb{H}, \langle \cdot, \cdot \rangle_{\mathbb{H}})$ be a reproducing kernel Hilbert space on \mathbb{R} with reproducing kernel $\mathcal{K} : \mathbb{R} \times \mathbb{R} \rightarrow \mathbb{R}$ and unit ball $\mathbb{H}_1 := \{f \in \mathbb{H} : \langle f, f \rangle_{\mathbb{H}} \leq 1\}$. For each $\theta \in \mathbb{R}$ denote by $\mathcal{K}_{\theta} \in \mathbb{H}$ the function $\mathcal{K}(\theta, \cdot)$, that satisfies $\langle \mathcal{K}_{\theta}, h \rangle_{\mathbb{H}} = h(\theta)$ for all $h \in \mathbb{H}$. The set $\mathcal{P}_{\mathcal{K}} := \{\text{Borel probability measures } \mu \text{ on } \mathbb{R} \text{ s.t. } \int_{\mathbb{R}} \sqrt{\mathcal{K}(\theta, \theta)} \mu(d\theta) < \infty\}$ can be embedded into \mathcal{H} by the mapping $\mu \mapsto \mu^{\mathbb{H}} := \int_{\mathbb{R}} \mathcal{K}_{\theta} \mu(d\theta)$. This induces a pseudo-metric on $\mathcal{P}_{\mathcal{K}}$ by

$$d_{\mathcal{K}}(\mu_1, \mu_2) := \|\mu_1^{\mathbb{H}} - \mu_2^{\mathbb{H}}\|_{\mathbb{H}} = \sup_{h \in \mathbb{H}_1} \left| \int_{\Theta} h(\theta) (\mu_1 - \mu_2)(d\theta) \right| \quad (10)$$

[17, §2.3]. The kernel \mathcal{K} is called *characteristic* if (10) is in fact a metric, i.e. $d_{\mathcal{K}}(\mu_1, \mu_2) = 0$ if and only if $\mu_1 = \mu_2$. The Gaussian kernel $\mathcal{K}_G(\theta, \theta') = \exp(-|\theta - \theta'|^2)$ is characteristic, by the definition given in [25, §2.3], since for any non-zero signed measure μ ,

$$\begin{aligned} \int \int \mathcal{K}_G(\theta, \theta') \mu(d\theta) \mu(d\theta') &= \frac{1}{2\sqrt{\pi}} \int \int \left\{ \int \exp(i(\theta - \theta')z) e^{-z^2/4} dz \right\} \mu(d\theta) \mu(d\theta') \\ &= \frac{1}{2\sqrt{\pi}} \int \left| \int \exp(i\theta z) \mu(d\theta) \right|^2 e^{-z^2/4} dz > 0. \end{aligned}$$

We use the estimator described in [17] given by

$$\hat{d}_{\mathcal{K}} := \frac{1}{J_1(J_1 - 1)} \sum_i \sum_j \mathcal{K}_G(v_i, v_j) + \frac{1}{J_2(J_2 - 1)} \sum_i \sum_j \mathcal{K}_G(z_i, z_j) - \frac{2}{J_1 J_2} \sum_i \sum_j \mathcal{K}_G(v_i, z_j).$$

2.4 A first application: stock price data

We illustrate the method by applying it to log daily returns of the 30 securities that made up the Dow Jones Industrial average as of January 1, 2015 for the period 2000–2014. Transformation to log returns is common in finance, and negative values are associated with declines in asset prices. We put $\bar{y}(x) = \hat{F}_{Y(x,\cdot)}^{-1}(0.1)$, where $\hat{F}_{Y(x,\cdot)}^{-1}(\alpha)$ is the empirical α quantile for the log return series of asset j . We compute waiting times until the observed series goes *below* these thresholds, so we are interested in dependence in extreme price *decreases*, or asset price crashes. Point estimates $\hat{\gamma}_d$ for every asset pair using AD, KS, \mathcal{K}_G , and M for d are shown in Figure 1; in the case of $d = M$, we show the value of the t statistic with unequal variances. These images are asymmetric, as expected, since $\gamma_d(x_1, x_2) \neq \gamma_d(x_2, x_1)$ in general, underscoring the sensitivity of the method to the order in which extreme events occur. In addition to estimates of M, we also show statistical significance for testing $H_0 : M = 0$ at level 0.05. The testing indicators are not shown for AD because most of the pairwise tests are significant, and they are omitted for KS because the presence of ties renders the p -values inaccurate. Here and elsewhere, p -values are adjusted to obtain False Discovery Rate (FDR) control at level 0.05 using the procedure of Benjamini and Hochberg.

Clearly, the strength of dependence in price crashes varies considerably across the Dow components. Many of the pairs exhibiting the largest values of $\hat{\gamma}_d$ — indicating strong dependence— are easily anticipated. For example, among the strongest interactions is that between *cvx* (Chevron) and *xom* (Exxon-Mobil), in either order, two equities whose price is mainly driven by a single underlying factor: global oil prices. Other pairs exhibiting strong dependence are Verizon (*vz*) and AT&T (*t*) and J.P. Morgan Chase (*jpm*) and Goldman Sachs (*gs*).

Histograms of each of the four statistics across all asset pairs are shown in Figure 2. It is clear from these plots that while the p values for testing $AD = 0$ and $KS = 0$ do not provide a useful way to identify interesting asset pairs, one can easily identify asset pairs with unusually strong dependence by selecting those with statistics in the right tail of the distribution.

2.5 Comparison to the Pickands dependence function

A popular functional measure of extremal dependence is the bivariate dependence function of Pickands [27] (see also Beirlant et al. [3, §8.2.5]). For a random n -vector Y following a max-stable distribution with distribution function G , define

$$\ell(v) := -\log G\{G_1^{\leftarrow}(e^{-v_1}), \dots, G_n^{\leftarrow}(e^{-v_n})\}$$

for $v \in \mathbb{R}_+^n$. The function $\ell(v)$ is the *stable tail dependence function* of G (see [3, p 257]). In the spatio-temporal setting, the random variables Y_1, \dots, Y_n are associated with the process at a collection of points, so $Y_i = Y(x_i, t)$, and repeated observations of the random vector Y correspond to sampling of the process at these locations at times t_1, \dots, t_J . The *Pickands dependence function* $A(r)$ is the restriction of the bivariate tail dependence function to the simplex

$$A(r) = \ell(1 - r, r), \quad r \in [0, 1]. \quad (11)$$

A bivariate max-stable distribution G is determined by its margins G_1, G_2 and A by

$$G(y_1, y_2) = \exp \left[\log\{G_1(y_1)G_2(y_2)\} A \left(\frac{\log\{G_2(y_2)\}}{\log\{G_1(y_1)G_2(y_2)\}} \right) \right].$$

Clearly, if $A = 1$, we obtain independence, while if A achieves its lower bound $A \leq (1 - r) \vee r$, we obtain $G(y_1, y_2) = G_1(y_1) \wedge G_2(y_2)$, which corresponds to complete dependence.

There is no direct representation of time in (11), but if $Y_1 = Y(x_1, t_1)$ and $Y_2 = Y(x_1, t_2)$, then A is a measure of dependence for a max-stable process at location x_1 at time t_1 and location x_2 at time t_2 . Clearly, the existence of a pair $\{(x_1, t_1), (x_2, t_2)\}$ for which $Y(x_1, t_1)$ is not independent of $Y(x_2, t_2)$ is sufficient for the distribution of waiting times between exceedances of y_1 at x_1 and y_2 at x_2 to differ from its distribution under complete independence. Conversely, if the distribution of waiting times between exceedances of y_1 at x_1 and y_2 at x_2 differs from its distribution under independence, then there must exist at least one pair $\{(x_1, t_1), (x_2, t_2)\}$ for which $A(r) \neq 1$. While a complete understanding of the temporal nature of dependence between locations x_1 and x_2 depends

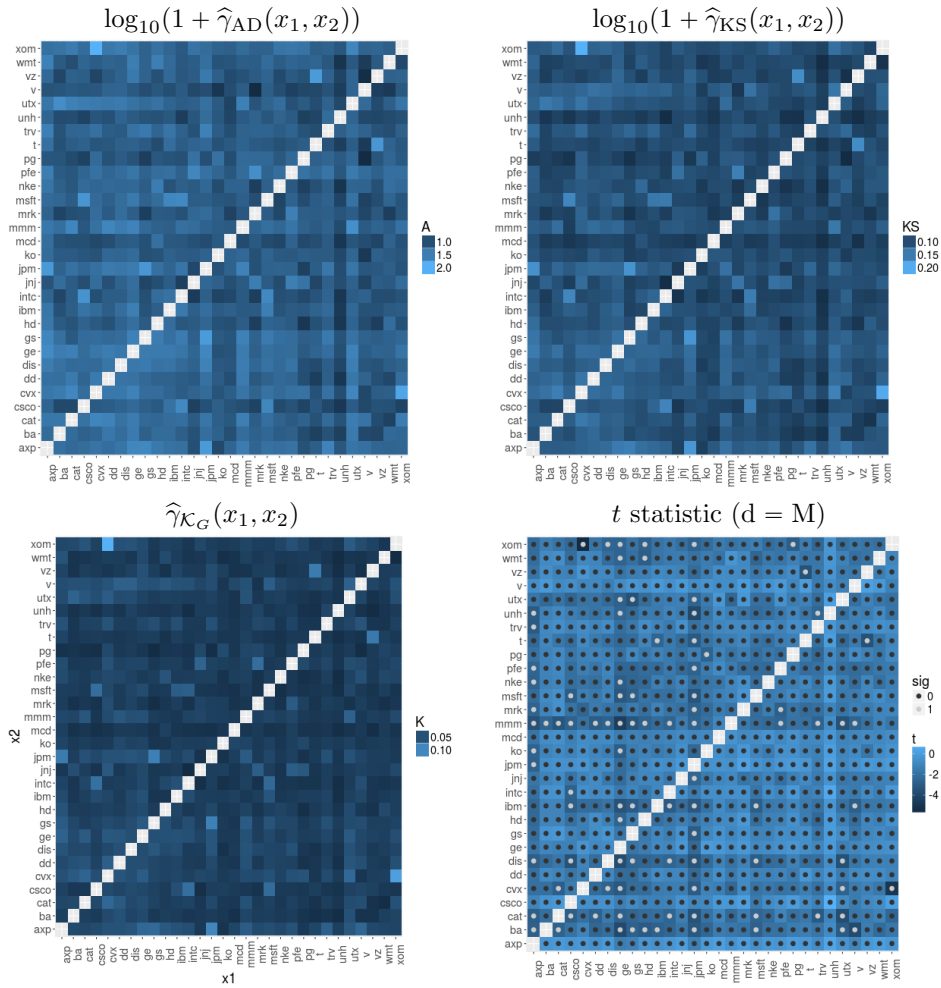


Figure 1: Results for DJIA data. Point estimates for each of the different metrics are shown by shading in tile plots. $\hat{\gamma}_{AD}$ and $\hat{\gamma}_{KS}$ are shown on the log scale for increased contrast. Statistical significance is shown by overlaid points on the graphic showing t statistics.

on A corresponding to every pair $\{(x_1, t_1), (x_2, t_2)\}$, it can be fully captured by γ_d in (4), at least for processes that are stationary in time. Moreover, while A only makes sense for max-stable processes, γ_d is meaningful for any space-time indexed stochastic process.

3 Waiting time distributions in a model of a max-stable process

In this section we construct a model of a space-time indexed max-stable process and derive some of its properties. Our goal is to connect the existing literature on the statistics of multivariate extremes with the proposed method by deriving distributions of waiting times in a model of a max-stable process. We also show that under this model, the sample means of waiting times satisfy a central limit theorem, and give a stochastic dominance result for Z that implies the mean waiting times are systematically shorter under dependence. We refer to the model as a *max-stable velocity process*. It is related to the space-time versions of the Gaussian max-stable model proposed by Davis et al. [10] and the general Markovian max-stable models of [15].

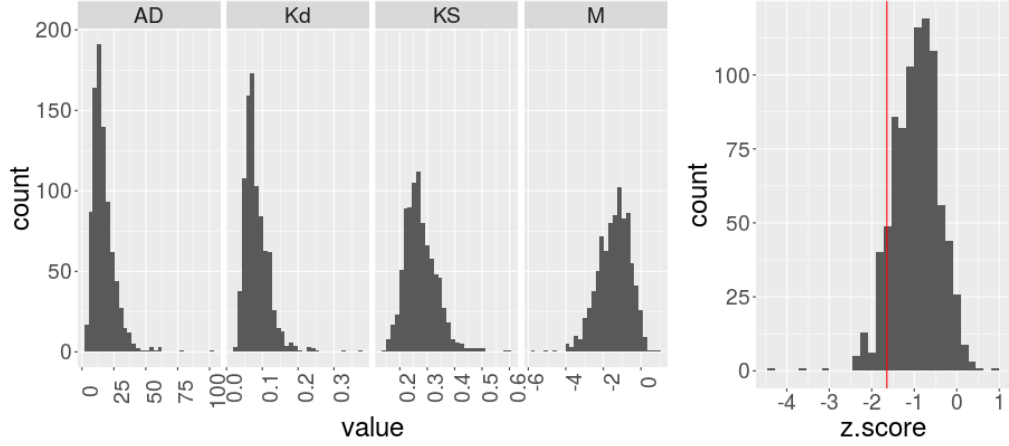


Figure 2: Left: histograms of raw statistics $\hat{\gamma}_d$ for $d = \text{AD}$, $d = \text{K}_G$ (labeled Kd), $d = \text{KS}$, and $d = \text{M}$ computed for every pair of assets; Right: histogram of z scores for testing $H_0 : M = 0$ after adjusting to control FDR at level 0.05.

3.1 Max-stable velocity processes

The max-stable velocity process is constructed by extending the spectral characterization of de Haan [12] and its continuous-path extension by Resnick and Roy [29]:

Theorem 3.1 (after de Haan and Resnick and Roy). *Let $\{(u_j, \xi_j)\}_{j \geq 1}$ be the points of a Poisson process on $\mathbb{R}_+ \times \mathbb{R}^d$ with intensity measure proportional to $u^{-2} du d\xi$. Let $\{Y(x)\}_{x \in \mathbb{R}^d}$ be a path-continuous max-stable process with unit Fréchet margins. Then there exist nonnegative continuous functions $\{k(x, \xi) : x, \xi \in \mathbb{R}^d\}$ such that*

$$\int_{\mathbb{R}^d} k(x, \xi) d\xi = 1 \quad \forall x \in \mathbb{R}^d$$

for which

$$\{Y(x)\}_{x \in \mathbb{R}^d} \stackrel{\mathcal{D}}{=} \left\{ \sup_{j \geq 1} u_j k(x, \xi_j) \right\}_{x \in \mathbb{R}^d}, \quad (12)$$

where $\stackrel{\mathcal{D}}{=}$ denotes equality in distribution. Moreover, any process defined by the right side of (12) is max-stable.

A useful heuristic for de Haan’s spectral characterization is that of weather extremes: the locations $\{\xi_j\}$ of the support points are taken to be storm centers, the kernel functions $k(x, \xi_j)$ describe the shape of the storm, and the marks $\{u_j\}$ quantify storm severity. In this context, the process realization is the maximum over some period of time of a climatological quantity, such as precipitation or temperature. To create a time-indexed process, we endow the points ξ_j with birth times, lifetimes, velocities, and shapes. This approach has the advantage of easily extending the physical interpretation of the points ξ_j as storms or, more generally “events.” Now, the storms will move and have finite lifespans.

Specifically: fix positive numbers $\beta > 0$ and $\delta > 0$ and a Borel probability measure $\pi(da)$ on a Polish “attribute space” \mathcal{A} . Define a σ -finite Borel measure

$$\nu(d\omega) := \beta u^{-2} du d\xi d\sigma d\tau d\pi(da) \quad (13)$$

on the space $\Omega := \mathbb{R}_+ \times \mathbb{R}^d \times \mathbb{R} \times \mathbb{R}_+ \times \mathcal{A}$, and let $\mathcal{N}(d\omega) \sim \text{Po}(\nu(d\omega))$ be a Poisson random measure on Ω with intensity $\nu(d\omega)$ — i.e., a measure that assigns independent random variables $\mathcal{N}(B_j) \sim \text{Po}(\nu(B_j))$ to disjoint Borel sets $B_j \subset \Omega$. Fix a nonnegative function $k : \mathbb{R}^d \times \mathbb{R} \times \mathbb{R}_+ \times \mathbb{R}_+ \times \mathcal{A} \rightarrow \mathbb{R}_+$ that satisfies $\int_{\mathbb{R}^d} k(x, t; \xi, \sigma, \tau, a) d\xi = 1$ for each x, t, σ, τ, a . Using the climatological heuristic, the support points $\{\omega_j\} = \{(u_j, \xi_j, \sigma_j, \tau_j, a_j)\}$ of $\mathcal{N}(d\omega)$ can be thought

of as representing storms of magnitudes $u_j > 0$, initiating at locations $\xi_j \in \mathbb{R}^d$ at times $\sigma_j \in \mathbb{R}$, with lifetimes $\tau_j \in \mathbb{R}_+$ and attribute vectors a_j that may include velocities v_j , shapes Λ_j , or other features. For any location $x \in \mathbb{R}^d$ and time $t \in \mathbb{R}$, define

$$Y(x, t) := \sup_j \{u_j k(x, t; \xi_j, \sigma_j, \tau_j, a_j)\} \quad t \in \mathbb{R} \quad (14a)$$

$$Y^*(x, t) := \sup_{0 \leq s \leq t} Y(x, s), \quad t \geq 0. \quad (14b)$$

We refer to (14a) as a *max-stable velocity (MSV) process* and (14b) as the corresponding *maximal MSV process*.

In the sequel we will take $\mathcal{A} = (\mathbb{R}^d \times \mathcal{P}^d)$ with elements $a_j = (v_j, \Lambda_j) \in \mathcal{A}$ that consist of a velocity vector $v_j \in \mathbb{R}^d$ and a shape matrix $\Lambda_j \in \mathcal{P}^d$, an element of the cone \mathcal{P}^d of positive-definite $d \times d$ matrices. Let $\varphi : \mathbb{R}^d \rightarrow \mathbb{R}_+$ be a continuous pdf satisfying $\int_{\mathbb{R}^d} \varphi(z) dz = 1$ that is non-increasing in $z'z$ and, for $\Lambda \in \mathcal{P}^d$, set $\varphi_\Lambda(z) := |\Lambda|^{1/2} \varphi(\Lambda^{1/2} z)$ (here $|\Lambda|$ denotes the determinant of $\Lambda \in \mathcal{P}^d$). We take k to have the specific form

$$k(x, t; \xi, \sigma, \tau, a) = \varphi_\Lambda(x - \xi - v(t - \sigma)) \mathbf{1}_{\{\sigma \leq t < \sigma + \tau\}}, \quad (15)$$

the magnitude at time t and location $x \in \mathbb{R}^d$ of a storm of unit severity that originated at location $\xi \in \mathbb{R}^d$ at a time $\sigma < t$ and moved at velocity $v \in \mathbb{R}^d$ for time $(t - \sigma)$. We write $Y \sim \text{MSV}(\beta, \delta, \pi, \varphi)$ to denote a process of the form (14a) with k defined by (15) and $\nu(d\omega)$ as in (13). This includes and generalizes the Gaussian and Student t kernels proposed as models for the generic max-stable process by Smith [34].

3.2 Main results

Max-stable velocity processes are in fact space-time indexed forms of the max-stable process, as shown in Theorem 3.2. All proofs are deferred to the Appendix.

Theorem 3.2 (Max-stable velocity processes are max-stable). *If $Y \sim \text{MSV}(\beta, \delta, \pi, \varphi)$, then Y is max-stable jointly in (x, t) on the index set $\mathbb{R}^d \times \mathbb{R}_+$.*

Theorem 3.2 is shown by verifying the definition in (1) directly— that is, by verifying that the process is “stable” under finite maxima. It turns out that the maximal MSV process $Y^*(x, t)$ of (14b) is also max-stable.

Theorem 3.3 (Maximal MSV process is max-stable). *If $Y \sim \text{MSV}(\beta, \delta, \pi, \varphi)$, then $Y^*(x, t)$ is max-stable in (x, t) on the index set $\mathbb{R}^d \times \mathbb{R}_+$.*

Therefore, if data are generated from a MSV process and transformed by taking blockwise maxima, the transformed data are realizations of a max-stable process.

The advantage of this particular max-stable process for our purposes is that waiting time distributions are fairly tractable. Theorem 3.4 gives the marginal distribution of the max-stable velocity process $Y(x, t)$ and that of the waiting times $V(x)$ until first exceedance.

Theorem 3.4 (Marginals and waiting times). *The max-stable velocity process has unit Fréchet marginals, with distribution function $P[Y(x, t) \leq y] = e^{-\beta/\delta y}$ for $y > 0$. The marginal waiting time distribution is given for $t \geq 0$ by*

$$P[V(x) > t] = \exp \left(-\frac{\beta}{\delta y} - t \frac{\beta}{\delta y} \left\{ \delta + \int_{\mathbb{R}^d \times \mathcal{P}^d \times v^\perp} \varphi_\Lambda(\zeta) d\zeta |v| \pi(dv d\Lambda) \right\} \right), \quad (16)$$

where $v^\perp := \{\zeta \in \mathbb{R}^d : v' \Lambda \zeta = 0\}$ denotes the orthogonal complement of the span of v in the Λ metric. This is a mixture of a point-mass at zero with weight $1 - \exp(\beta/\delta y)$ and an exponential distribution with a shape-dependent rate constant that increases monotonically in the mean particle speed.

The next result shows that $Z(x_1, x_2)$ and $V(x)$ obey the central limit theorem, and that the convergence rate will in most cases be uniform over all points in the index set. This implies that one can use two-sample t statistics to test $H_0 : M = 0$ for our procedure when the data originate from a MSV process.

Corollary 3.5. *The distribution of $Z(x_1, x_2)$ is stochastically dominated by a mixture of an exponential and an atom at zero. Therefore*

$$J^{-1} \sum_{j=1}^J z_j(x_1, x_2), \quad J^{-1} \sum_{j=1}^J v_j(x),$$

suitably centered and scaled, both obey the central limit theorem and converge to Gaussian in the Wasserstein-1 and Kolmogorov metrics. If further

$$\sup_{x \in \mathcal{X}} \int_{\mathbb{R}^d \times \mathcal{P}^d \times v^\perp} \varphi_\Lambda(\zeta) d\zeta |v| \pi(dv d\Lambda) < \infty, \quad (17)$$

then the convergence rate is uniform over all x .

Theorem 3.4 also gives immediately the distribution of Y^* .

Corollary 3.6 (Distribution of Y^*). *The distribution of $Y(x, t) = P[Y^*(x, t) < y]$ is given by (16).*

Thus the waiting time distribution and the distribution of $Y^*(x, t)$, unlike the marginal distribution of $Y(x, t)$, depends on velocity and shape. For Gaussian kernels φ , (16) has a simple expression:

Corollary 3.7 (Waiting time distribution for Gaussian kernels). *For Gaussian kernels $\varphi(z) = (2\pi)^{-d/2} \exp(-z'z/2)$,*

$$P[V(x) > t] = \exp \left(-\frac{\beta}{\delta y} - t \frac{\beta}{\delta y} \left\{ \delta + E_\pi \left[(v' \Lambda v / 2\pi)^{\frac{1}{2}} \right] \right\} \right). \quad (18)$$

Thus in the Gaussian case, the marginal waiting times converge to zero in distribution as $E_\pi[\sqrt{v' \Lambda v}] \rightarrow \infty$.

3.3 Results on multivariate marginals and $Z(x_1, x_2)$

We now give results on the joint distribution and the distribution of waiting times between exceedances. Theorem 3.8 gives the joint distribution of the max-stable velocity process at finite collections of locations $\{x_i\}_{1 \leq i \leq n}$ and times $\{t_i\}_{1 \leq i \leq n}$.

Theorem 3.8 (Joint CDF). *Let $Y \sim \text{MSV}(\beta, \delta, \pi, \varphi)$ be a max-stable velocity process and let $\{x_i\}_{1 \leq i \leq n} \subset \mathbb{R}^d$ and $\{t_i\}_{1 \leq i \leq n} \subset \mathbb{R}$ for some integer $n \in \mathbb{N}$. The joint CDF for $\{Y(x_i, t_i)\}_{1 \leq i \leq n}$ is given by*

$$F(y_1, \dots, y_n) := P(\cap_{1 \leq i \leq n} [Y(x_i, t_i) \leq y_i]) = \exp(-\nu(\cup_{1 \leq i \leq n} B_i)) \quad (19a)$$

for $B_i := \{\omega : Y(x_i, t_i) > y_i\}$, with

$$\nu(\cup_{1 \leq i \leq n} B_i) = \sum_{1 \leq i \leq n} \nu(B_i) - \sum_{i \neq j} \nu(B_i \cap B_j) + \sum_{i \neq j \neq k} \nu(B_i \cap B_j \cap B_k) - \dots, \quad (19b)$$

the alternating sum of terms

$$\nu(\cap_{i \in J} B_i) = \frac{\beta}{\delta} e^{-\delta(t^J - t_J)} \int_{\mathbb{R}^d \times \mathcal{A}} \min_{j \in J} \left\{ \frac{\varphi_\Lambda(x_j - vt_j - z)}{y_j} \right\} dz \pi(dv d\Lambda) \quad (19c)$$

for subsets $J \subseteq \{1, \dots, n\}$. Here $t^J := \max\{t_j\}$ denotes the maximum and $t_J := \min\{t_j\}$ the minimum of $\{t_j\}_{j \in J}$.

While the univariate marginal distributions of $Y(x, t)$ do not depend on $\pi(dv d\Lambda)$ at all, higher order marginal distributions do. For example,

Corollary 3.9 (Gaussian MSV process joint CDF at two points). *For the Gaussian max-stable velocity process with $\varphi(z) = (2\pi)^{-d/2} \exp(-z'z/2)$, the bivariate distribution is given for $y_1, y_2 > 0$ by $F(y_1, y_2) = \exp(-\nu(B_1 \cup B_2))$ with*

$$\begin{aligned} \nu(B_1 \cup B_2) &= \frac{\beta}{\delta} \left(1 - e^{-\delta|t_2 - t_1|}\right) \left(\frac{1}{y_1} + \frac{1}{y_2}\right) + \frac{\beta}{\delta} e^{-\delta|t_2 - t_1|} \\ &\times \int_{\mathcal{P}^d \times \mathbb{R}^d} \left\{ \frac{1}{y_1} \Phi\left(\frac{S_\Lambda(v)}{2} - \frac{\log(y_1/y_2)}{S_\Lambda(v)}\right) + \frac{1}{y_2} \Phi\left(\frac{S_\Lambda(v)}{2} - \frac{\log(y_2/y_1)}{S_\Lambda(v)}\right) \right\} \pi(dv d\Lambda) \end{aligned} \quad (20)$$

where $\Phi(\cdot)$ is the standard Gaussian CDF and $S_\Lambda(v) := \sqrt{\Delta_v' \Lambda \Delta_v}$ for $\Delta_v := (x_2 - x_1) - (t_2 - t_1)v$.

Equation (20) generalizes Smith [34, equation 3.1], and reduces to it if $t_1 = t_2$ and if π is a unit point mass. It leads to an explicit expression for the likelihood function for the Gaussian max-stable velocity process with observations at two locations and times. This expression could be used to fit the max-stable velocity process to data by maximum composite likelihood.

Our final result is for the distribution of

$$Z^*(x_1, x_2) = |V(x_2) - V(x_1)|,$$

which is more convenient to study than $Z(x_1, x_2)$, since we need not be concerned about the order in which the exceedances occur. This considerably simplifies the construction of sets to integrate over in obtaining the following result. The subsequent corollary gives a stochastic ordering result for either $Z(x_1, x_2)$ or $Z(x_2, x_1)$ every $x_1, x_2 \in \mathcal{X}$. Results are given here for the Gaussian kernel; expressions for the general case can be found in the Appendix.

Theorem 3.10 (Stochastic bound for survival function with nonzero velocity). *Suppose $Y \sim \text{MSV}(\beta, \delta, \pi, \varphi)$ is a Gaussian max-stable velocity process. Then for any two points x_1, x_2 and thresholds y_1, y_2 , κ_Δ satisfies the stochastic ordering*

$$\mathbb{P}[Z^*(x_1, x_2) > t] \leq \exp\{-\nu(A)\},$$

with

$$\begin{aligned} \nu(A) &= \frac{\beta}{\sqrt{2\pi}} \int_{\mathbb{R}^d \times \mathcal{P}^d} (t - \Delta_{12}) e^{-\delta \Delta_{12}} \left\{ \frac{1}{y_1} \Phi\left(-\frac{S_\Lambda^\perp(v)}{2} + \frac{\log(y_1/y_2)}{S_\Lambda^\perp(v)}\right) \right. \\ &\quad \left. + \frac{1}{y_2} \Phi\left(-\frac{S_\Lambda^\perp(v)}{2} - \frac{\log(y_1/y_2)}{S_\Lambda^\perp(v)}\right) \right\} \sqrt{v' \Lambda v} \pi(d\Lambda dv), \end{aligned} \quad (21)$$

where $S_\Lambda^\perp(v) := \{(x_2 - x_1)' \Lambda (x_2 - x_1)^\perp\}^{1/2}$, $\Delta_{12} := v' \Lambda (x_2 - x_1) / v' \Lambda v$, and $(x_2 - x_1)^\perp := (x_2 - x_1) - \Delta_{12}v$ is the projection of $(x_2 - x_1)$ into the orthogonal complement of v in the Λ metric.

Corollary 3.11. *At least one of*

$$\mathbb{P}[Z(x_1, x_2) > t] \leq \exp\{-\nu(A)/2\}$$

or

$$\mathbb{P}[Z(x_2, x_1) > t] \leq \exp\{-\nu(A)/2\}$$

holds. Also

$$\mathbb{P}[Z(x_1, x_2) \wedge Z(x_2, x_1) > t] \leq \exp\{-\nu(A)/2\}.$$

Theorem 3.10 shows that for the Gaussian MSV process, $Z^*(x_1, x_2)$ – and at least one of $Z(x_1, x_2)$ and $Z(x_2, x_1)$ – converges to zero in probability if

$$\mathbb{E}_\pi \left[\sqrt{v' \Lambda v} \Phi \left(-\sqrt{(x_2 - x_1)' \Lambda (x_2 - x_1)^\perp} \right) \right] \rightarrow \infty.$$

This condition is only slightly stronger than the condition $\mathbb{E}_\pi[\sqrt{v'\Lambda v}] \rightarrow \infty$, which is sufficient for the marginal waiting times to converge to zero in probability based on (18). Informally, the difference between these conditions is that $\pi(dv d\Lambda)$ cannot place too much mass on Λ with large eigenvalues, which corresponds to extremely concentrated kernels. This is intuitive: it is difficult for the same point to cause an exceedance at two different locations when the kernels are extremely concentrated, since the volumes of space where exceedances can occur are very small. This result and Theorem 3.4 together imply that the waiting time distributions are stochastically decreasing in mean speed, and the distribution of $Z(x_1, x_2)$ is dominated by a mixture of an atom at zero and an exponential distribution. Moreover, the stochastic ordering also implies that at least one of $\mathbb{E}[Z(x_1, x_2)]$ and $\mathbb{E}[Z(x_2, x_1)]$ is decreasing in mean speed, so the use of M for d in defining γ_d is in some cases reasonable.

4 Simulation

In this section, a simulation study is constructed to illustrate the method. We simulate from a MSV process and then perform inference using our waiting time-based procedure. The simulation is motivated by extreme weather events, where basic scientific knowledge allows informative choices. Data are simulated from a Gaussian max-stable velocity process with attribute distribution

$$\begin{aligned} \pi(da) = \pi(dr d\phi d\Lambda) &\propto |\Lambda|^{(\nu-k-1)/2} e^{-\text{tr}(\Psi^{-1}\Lambda)/2} r^{-3/2} e^{-(a(r-m)^2)/(2m^2 r)} \\ &\times \prod_{h=1}^{k-1} \left[\frac{1}{2} q e^{-q\phi_h} \mathbf{1}_{\{\phi_h > 0\}} + \frac{1}{2} q e^{-q\phi_h} \mathbf{1}_{\{\phi_h < 0\}} \right] dr d\phi d\Lambda, \end{aligned}$$

where $(r, \phi_1, \dots, \phi_{k-1})$ is the polar parametrization of the velocity v . This corresponds to a Wishart distribution for Λ with degrees of freedom ν and shape Ψ , an inverse Gaussian distribution for the magnitude of the velocity r with parameters m, a , and wrapped Laplace distributions with parameter q for the angles $(\phi_1, \dots, \phi_{k-1})$ defining the direction of the velocity in \mathbb{R}^k . The storm lifetimes $\tau \sim \text{Exponential}(\delta)$ and the support points ξ follow a homogeneous spatial Poisson process with rate $\beta d\xi$. The intensity measure in the specification of the process $u \propto u^{-2}$ is improper. For the simulation, we put $u \sim \text{Pareto}(u_{\min}, 1)$, the conditional distribution of u given $u > u_{\min}$. Hyperparameters for the simulation, and their units, are shown in Table 1.

Table 1: Hyperparameter choices for simulations

	β	u_{\min}	δ	Ψ	ν	m	a	q
value	$1/(600)$	1	$1/120$	I_2	7	$1/10$	$1/2$	$1/2$
units	$(500^2 \text{ km}^2 \text{ hr})^{-1}$	–	hr^{-1}	500^2 km^2	–	500 km hr^{-1}	500 km hr^{-1}	–

The data are simulated on a 10×10 box B . In order to inform hyperparameter choices, this box is taken to roughly represent a 5000^2 km^2 area containing the continental United States and southern Canada. As a result, the distributions of velocity and lifetimes of storms are chosen to approximate the behavior of weather events in this geographic region. To set the time scale and allow easier interpretation of results, one unit of time in the simulation is considered one hour. Support points of the marginal process $\mathcal{N}(d\xi d\sigma)$ are sampled on $B \times [0, T]$, with $T = 114 \times 365 \times 24 = 998\,640$, so that the number of support points of $\mathcal{N}(d\xi d\sigma)$ are Poisson distributed with mean $\beta \times T \times 100 (500^2 \text{ km}^2 \text{ hr})^{-1}$. The choice of $\beta = 1/600 (500^2 \text{ km}^2 \text{ hr})^{-1}$ gives an average of four storms a day forming in the region. Storm lifetimes τ_j are sampled for each support point from $\text{Exponential}(1/120)$, which gives an average storm lifetime of five days. Intensities, shapes, and velocities are sampled from the specified distributions with the hyperparameters given in Table 1. The values $m = 0.1, a = 1/2$ for the inverse Gaussian distribution on r gives an average speed of about 50 km hr^{-1} . The parameter $q = 0.5$ places most of the mass on easterly storm tracks.

The value of the process $Y(x, t)$ is recorded at one million homogeneously spaced time points from $[0, T]$ at the five locations $\{x_1 = (5, 5), x_2 = (5, 5.5), x_3 = (1, 1), x_4 = (8, 8), x_5 = (3, 5)\}$, as well as twenty additional locations sampled uniformly on B . The five fixed points should result in the process at some pairs of locations being highly tail dependent, some pairs weakly dependent, and some nearly independent. After simulation, waiting times between exceedances

of $y(x) = \hat{F}_{Y(x,\cdot)}^{-1}(0.995)$ are calculated at every unique pair of points. We then estimate γ_d for $d = \text{AD}, \text{KS}, \mathcal{K}_G$, and M . Plots of $\hat{\gamma}_d$ against Euclidean distance between pairs of points are shown in Figure 3. As expected, $\hat{\gamma}_d(x_1, x_2)$ is decreasing in $\|x_1 - x_2\|_2$. For the t statistic, decreasing $\gamma_d(x_1, x_2)$ corresponds to a decrease in the absolute value of the statistic, which is what we observe. Throughout, we show the raw t statistic instead of its absolute value since the t statistic is negative when $\mathbb{E}[Z(x_1, x_2)] < \mathbb{E}[V(x_2)]$. As expected based on Theorem 3.10, the sign of the t statistic tends to be negative when $\|x_1 - x_2\|_2$ is small, but is equally likely to be positive or negative when $\|x_1 - x_2\|_2$ is large. In addition, noticeable differences are observed between the behavior of $\hat{\gamma}_d$ with $d = \text{AD}$, $d = \text{KS}$, and $d = \mathcal{K}_G$ as a function of distance. In particular, when $d = \text{KS}$, the statistic is somewhat noisier as a measure of dependence.

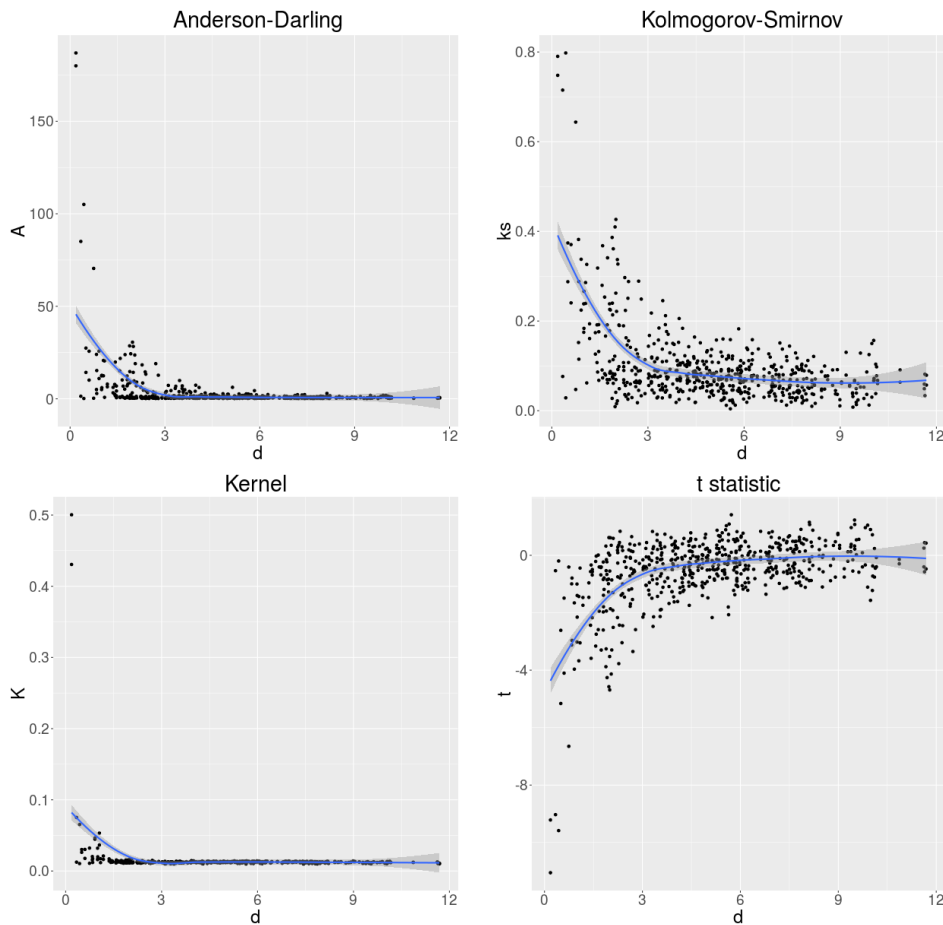


Figure 3: $\hat{\gamma}_d(x_1, x_2)$ as a function of $\|x_1 - x_2\|_2$ for different choices of d . Results for \mathcal{K}_G are labeled “Kernel,” and t statistics are shown rather than $d = \text{M}$.

5 Applications

The method is applied to three additional real data sets: (1) Daily precipitation data for 25 weather stations in the United States for the period 1940–2014; (2) Daily exchange rates for 12 currencies for the period 1986–1996; and (4) Electrical potential at 62 single neurons in the brain of a mouse exploring a maze, sampled at 500 Hz.

The first dataset is similar to the simulation study and the physical heuristic that we introduced in Section 3. The third—the mouse electrophysiology data—retains an explicit spatial component, as the physical distance between neurons is related to the speed at which signals can be propagated between them. The second application, like the Dow Jones application in Section 2.4, is financial.

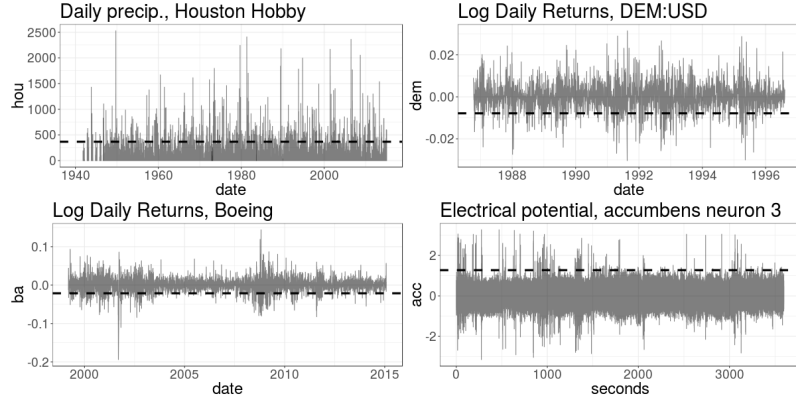


Figure 4: Examples of raw data $y(x, t)$. Dashed lines show $\bar{y}(x)$. The electrophysiology data are downsampled by a factor of 100.

In these applications, the “spatial” index \mathcal{X} can be thought of as a coordinate in a latent “attribute” space, with the distances between assets reflecting similarity in the factors that determine their price. No explicit reference to the index set \mathcal{X} is necessary, however, to make the waiting times between threshold exceedances meaningful. In financial settings, these reflect the speed with which sentiment about particular asset classes propagates through the market. Note that in financial settings it is usually extremes in the *left* tail that are of particular interest, and thus it is useful to model with max-stable velocity processes the negative of the observed data—so exceedances of the negative of a low threshold are the relevant events.

In choosing thresholds $\bar{y}(x)$ for analysis, the heuristic used is that

$$\min_{x_1, x_2 \in \mathcal{X}^s \times \mathcal{X}^s} \#\{z_j(x_1, x_2)\} \geq 75 \quad (22)$$

where the set $\{z_j(x_1, x_2)\}$ is obtained using the procedure in (8), $\#A$ for a set A indicates the cardinality of A , and \mathcal{X}^s is the set of spatial locations at which the process is sampled. Thresholds correspond to empirical quantiles of the observed data, and the same threshold is used for $\bar{y}(x_1)$, $\bar{y}(x_2)$ in both the procedure for estimation of $\mathcal{L}(V(x_1))$ and $\mathcal{L}(V(x_2))$ and that for estimation of $\mathcal{L}(Z(x_1, x_2))$. We always use the empirical median for $y(x)$. A consequence of choosing thresholds in this way is that for some datasets, the empirical quantile of the chosen threshold may be much more extreme than for others. For example, the electrophysiology data has nearly two million observations, so we can choose a threshold of $\bar{y}(x) = \hat{F}_{Y(x, \cdot)}^{-1}(0.995)$ for analysis; the exchange rate data has only about two thousand observations, so the threshold chosen is $y_i = \hat{F}_{Y(x, \cdot)}^{-1}(0.90)$. For the Dow Jones data, extensive temporal clustering of extreme events results in the highest possible threshold that satisfies (22) being $y(x) = \hat{F}_{Y(x, \cdot)}^{-1}(0.90)$. For the precipitation data, the threshold used is $y(x) = \hat{F}_{Y(x, \cdot)}^{-1}(0.975)$. Examples of single components of the four datasets are shown in Figure 4. In the case of the two financial datasets, the displayed series and data used for our analysis are the log daily returns $\log[y(x, t)/y(x, t-1)]$, following standard practice in finance. The other two figures show the raw data plotted in the time domain.

5.1 Precipitation

Results for analysis of the precipitation data are summarized in Figure 5. A map showing the location of each station can be found in Figure 9 in the Appendix. Clear geographic structure is evident in the estimated values of $\gamma_d(x_1, x_2)$. Overall, tail dependence is evident at nearby sites but decays with distance; for distances greater than about 500 km the estimated values of γ_d are all very similar. Particularly strong dependence is observed between two nearby cities in California: San Francisco and Sacramento. Extremely high dependence exists between two sites both located in Sacramento. There is noticeable difference between the observed dependence structure when KS is used compared to AD. Of the $25^2 - 25 = 500$ estimated statistics $\hat{\gamma}_d(x_1, x_2)$ with $d = M$, only 21

were statistically significant. These include every combination of the two sites in Sacramento and the site in San Francisco in either temporal order, and several other sensible pairs like Baltimore and Washington, and New York and Boston. The results are largely consistent with background knowledge about weather patterns in the United States and the relative proximity and spatial orientation of these sites. Also shown is a plot of $\hat{\gamma}_d(x_1, x_2)$ vs $\|x_1 - x_2\|_2$ with $d = \text{KS}$. The expected pattern of decreasing dependence at increasing distance is seen.

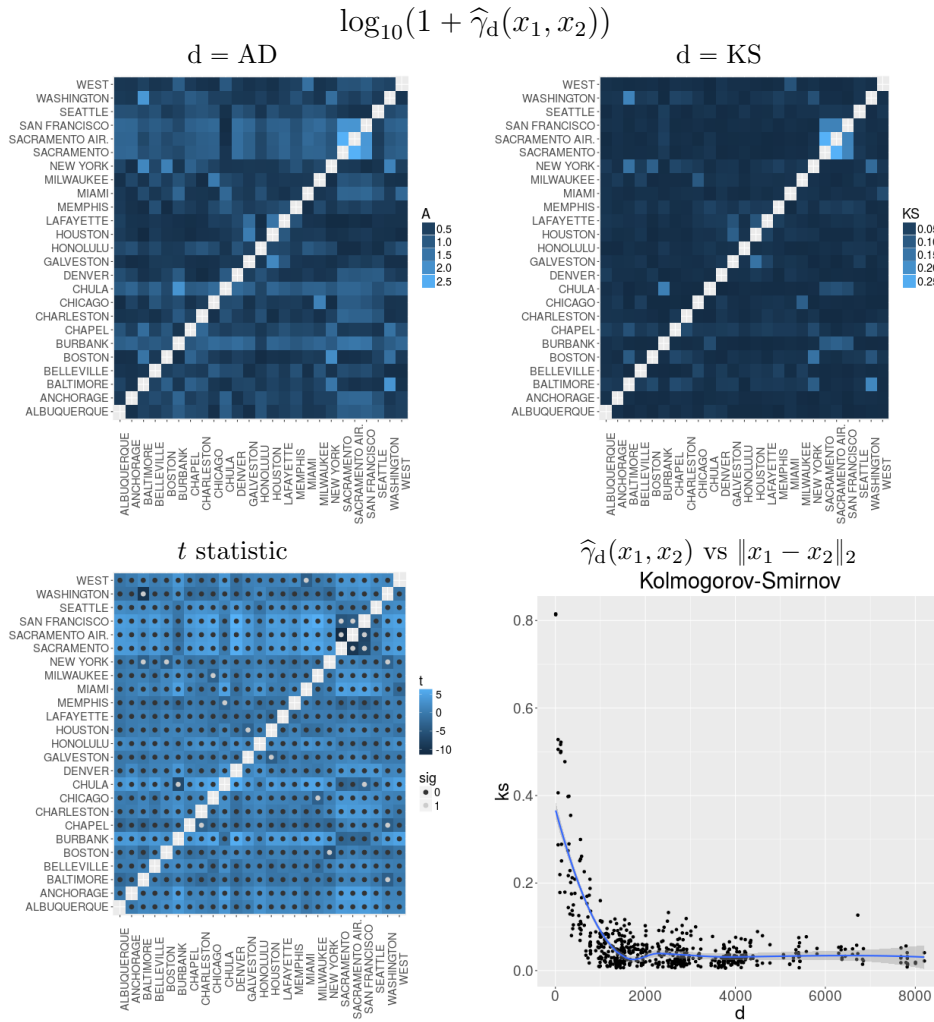


Figure 5: Results for daily precipitation data as described in text. The values of $\hat{\gamma}_d(x_1, x_2)$ for $d = \text{KS}, \text{AD}$ in the top two panels are shown on the log scale for improved contrast. Overlaid dots on t statistic graphic show significance at the 0.05 level after adjusting for multiplicity (light dot: $p < 0.05$).

5.2 Exchange Rates

Exchange rate data for twelve currencies is described in [20] and [28]. A table giving the full name of each currency and its corresponding row/column in the color map is provided in Table 2 in the Appendix. Figure 6 shows some results. Here, there is very clear structure in the pattern of pairwise dependence, with the European currencies (BEF, FRF, DEM, NLG, ESP, SEK, CHF, and GBP) showing strong evidence of dependence while the other four currencies (AUD, CAD, JPY, and NZD) show little evidence of tail dependence among themselves or with the European currencies. Order matters as well; for example, SEK is highly dependent in one direction but not the other. About one third of the $12^2 - 12 = 132$ pairs exhibit statistically significant tail dependence with $d = \text{M}$.

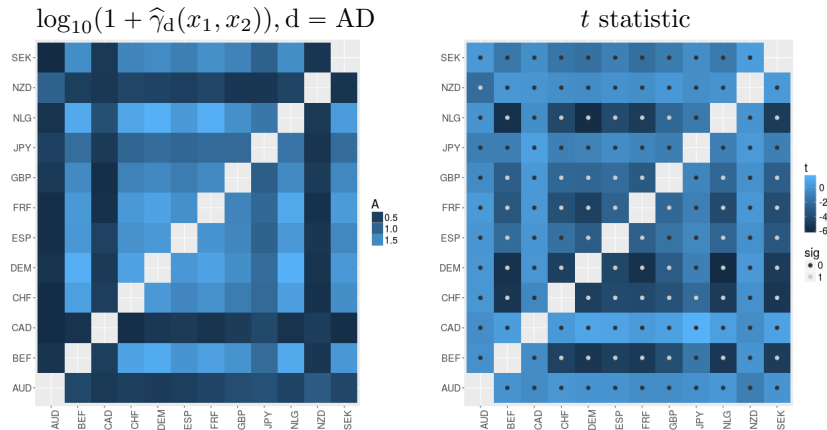


Figure 6: Results for exchange rate data as described in text.

5.3 Electrophysiology

Potential data recorded at single neurons in the brain of a mouse interacting with a maze are described in [14]. In electrophysiology, interest lies in modeling dependence between neuron “spikes” at different locations in the brain. Neuronal voltage spikes indicate transmission of signals along axonal pathways, and large potentials tend to cluster together in small time windows. These events are referred to as “spike trains.” Thus, in these data one expects to see extensive tail dependence, but the waiting times between spikes at different neurons are relevant, since they inform about the pathway that the signal takes through the brain.

The neurons are assigned to regions of the brain, which are labeled in Figure 7. There is ample evidence of strong tail dependence for many pairs of neurons, but the matrix of $\hat{\gamma}_d(x_1, x_2)$ is highly asymmetric, indicating that spikes in some regions tend to follow spikes in other regions. This is consistent with the basic understanding of how signals are propagated through the brain. For space reasons, we only show results for $d = AD$ here. Figure 8 shows a histogram of the p values for testing $H_0 : \hat{\gamma}_d(x_1, x_2) = 0$ with $d = M$ using the t test with unequal variances, adjusted using the method of Benjamini and Hochberg. It is clear that even in this setting where dependence is very high, it is possible to separate more and less scientifically interesting pairs using this method. Performing the tests at the level of brain region instead of individual neuron might give more power, at the cost of spatial resolution.

6 Discussion

Characterizing tail dependence based on waiting times between peaks over thresholds has the advantage of greater flexibility and generality than existing alternatives in cases where temporal lags in extreme events are possible. The method relies strictly on the waiting times and inference on the parameter $\gamma_d(x_1, x_2)$, and is relatively simple and computationally scalable compared to fitting models of max-stable processes to data. The inferential method based on waiting times is robust to misspecification of the underlying process as long as the method selected for estimation of the waiting time distributions is sufficiently flexible. Here we have opted for nonparametric methods to avoid misspecification problems; where significant domain knowledge is available, power could be gained by using parametric methods to estimate $\mathcal{L}(V(x))$ and $\mathcal{L}(Z(x_1, x_2))$.

Like other peaks-over-thresholds methods, our approach requires the choice of appropriate thresholds. Substantial work has been done on threshold choice for standard peaks-over-thresholds methods. It is unclear whether this will translate directly to threshold choice in the waiting times context. We have taken the simpler approach of choosing a threshold to achieve a minimum number of data points. Further work on threshold choice is called for. Additionally, we have thus far modeled the pairwise waiting times entirely independently; clear gains in estimation efficiency would result from sharing information across all pairs. These are worthwhile areas for future work.

$$\hat{\gamma}_d(x_1, x_2), d = \text{AD}$$

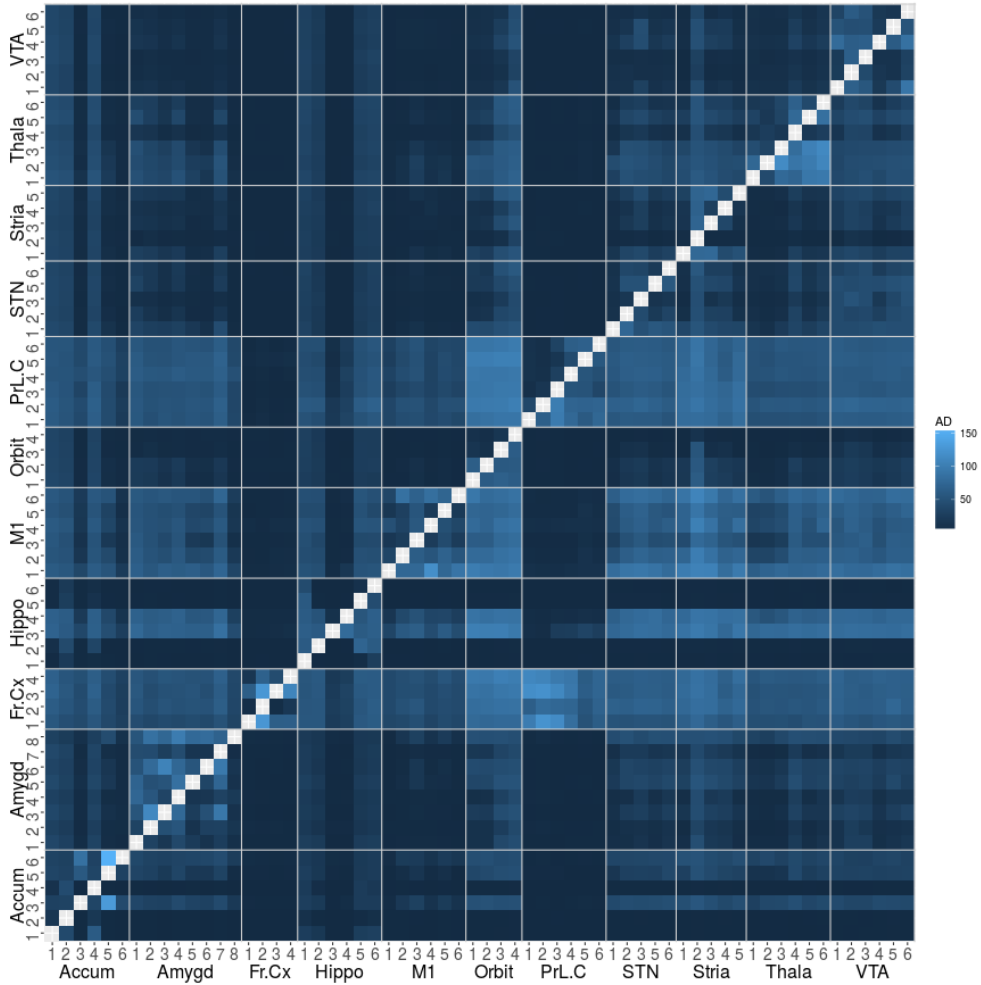


Figure 7: Results for electrophysiology application as described in text. The neurons are assigned to 11 different brain regions; the axis labels show the abbreviated brain region name and an identifier for the neuron within each region. Blocks of neurons within a single brain region are delineated by horizontal and vertical white lines.

Acknowledgments

The authors thank Dan Cooley and David Dunson for helpful comments on drafts of this manuscript, and Kristian Lum for assistance in obtaining data for the climatological applications. James Johndrow acknowledges funding from the United States National Institute of Environmental Health Sciences, grant numbers ES017436, ES020619, and ES017240, as well as the National Science Foundation and National Institutes of Health. Robert Wolpert acknowledges funding from United States National Science Foundation, grant numbers SES-1521855 and ACI-1550225.

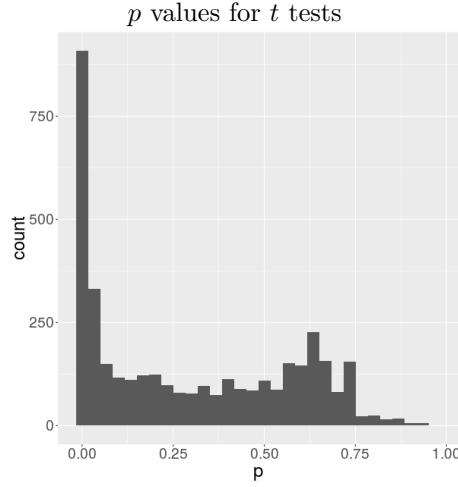


Figure 8: p values for t tests of difference in means between $Z(x_1, x_2)$ and $V(x_2)$ for electrophysiology data.

Appendix

A Proof of Theorems 3.2 and 3.3

A.1 Proof of Theorem 3.2

Theorem 3.2 is a corollary of the following result.

Theorem A.1 (Maxima of MSV Processes). *If $Y_i \stackrel{\text{iid}}{\sim} \text{MSV}(\beta, \delta, \pi, \varphi)$ are independent MSV processes for $1 \leq i \leq n$ then their maximum $\vee_{1 \leq i \leq n} Y_i(x, t) := \max_{1 \leq i \leq n} Y_i(x, t)$ is a max-stable velocity process with the $\text{MSV}(n\beta, \delta, \pi, \varphi)$ distribution.*

Proof. Each of $\{Y_i\}$ has a representation (14a) for the support points $\{\omega_j^{(i)}\}_{j \in \mathbb{N}}$ of the i th of n independent Poisson random measures $\mathcal{N}^{(i)}(d\omega) \stackrel{\text{iid}}{\sim} \text{Po}(\nu(du))$ for the intensity measure $\nu(d\omega)$ of (13). Then their sum $\mathcal{N}^+(d\omega) := \sum_{1 \leq i \leq n} \mathcal{N}^{(i)}(d\omega) \sim \text{Po}(n\nu(du))$ is also a Poisson random measure, with intensity measure n times $\nu(d\omega)$ and with support equal to the union of the supports of $\{\mathcal{N}^{(i)}\}$. The MSV processes associated with \mathcal{N}^+ is precisely $\vee_{1 \leq i \leq n} Y_i(x, t)$, since

$$\begin{aligned} \mathbb{P}[\vee_{1 \leq i \leq n} Y_i(x, t) < y] &= \mathbb{P}[\cap_{i=1}^n \{Y_i < y\}] \\ &= \prod_{i=1}^n e^{-\nu(B)} = e^{-n\nu(B)}, \end{aligned}$$

for $B = \{Y_i < y\}$. But the measure $n \cdot \nu$ of (13) is exactly that of the $\text{MSV}(n\beta, \delta, \pi, \varphi)$ process. \square

We now prove Theorem 3.2.

Proof. Fix $Y \sim \text{MSV}(\beta, \delta, \pi, \varphi)$ and n iid max-stable copies $\{Y_i\}_{1 \leq i \leq n} \stackrel{\text{iid}}{\sim} \text{MSV}(\beta, \delta, \pi, \varphi)$. By Theorem A.1 the maximum $\vee_{1 \leq i \leq n} Y_i(x, t)$ has the $\text{MSV}(n\beta, \delta, \pi, \varphi)$ distribution. By (19) in Theorem 3.8, multiply β and each y_j by n to see that all finite-dimensional marginal joint distributions of $\{\vee_{1 \leq i \leq n} Y_i(x, t)\}$ are identical to those of $\{nY(x, t)\}$, so $Y(x, t) \stackrel{\mathcal{D}}{=} \frac{1}{n} \vee_{1 \leq i \leq n} Y_i(x, t)$ satisfies (1) of Theorem 3.1 and Y is max-stable. \square

A.2 Proof of Theorem 3.3

We first prove two lemmas used in obtaining the main result.

Lemma A.1. *If $Y_1 \sim \text{MSV}(\beta, \delta, \pi, \varphi)$ and $Y_c \sim \text{MSV}(c\beta, \delta, \pi, \varphi)$ for some $c > 0$, then $cY_1^* \stackrel{D}{=} Y_c^*$.*

Proof.

Fix $\{x_i\}_{1 \leq i \leq n} \subset \mathbb{R}^d$ and $\{t_i\}_{1 \leq i \leq n} \subset \mathbb{R}$. The joint CDF for $\{Y_1^*(x_i, t_i)\}$ at $\{y_i\} \subset \mathbb{R}_+$ is

$$P[\cap_{1 \leq i \leq n} [Y_1^*(x_i, t_i) \leq y_i]] = \exp(-\nu(\cup_{1 \leq i \leq n} A_i)) \quad (23)$$

for the exceedance events $A_i := [Y_1^*(x_i, t_i) > y_i]$, which may be written

$$A_i = \left\{ \omega : u > \frac{y_i}{\sup_{(0 \vee \sigma) \leq s \leq (t_i \wedge \sigma + \tau)} \{\varphi_\Lambda(x_i - \xi - v(s - \sigma))\}} \right\}.$$

By the inclusion-exclusion principle, $\nu(\cup A_i)$ can be evaluated as

$$\nu(\cup_{1 \leq i \leq n} A_i) = \sum_{\emptyset \neq J \subset \{1, \dots, n\}} (-1)^{1+|J|} \nu(\cap_{j \in J} A_j), \quad (24)$$

where $|J|$ denotes the cardinality of J . For a finite set $J \subset \{1, \dots, n\}$ of indices, the intersection

$$\cap_{j \in J} A_j = \left\{ \omega : u > \max_{j \in J} \left[\frac{y_j}{\sup_{(0 \vee \sigma) \leq s \leq (t_j \wedge \sigma + \tau)} \{\varphi_\Lambda(x_j - \xi - v(s - \sigma))\}} \right] \right\}$$

has ν -measure (after changing variables from ξ to $z := \xi + v\sigma$)

$$\nu\left(\cap_{j \in J} A_j\right) = \int \min_{j \in J} \left[\frac{\sup_{(0 \vee \sigma) \leq s \leq (t_j \wedge \sigma + \tau)} \{\varphi_\Lambda(x_j - vs - z)\}}{y_j} \right] dz \beta d\sigma \delta e^{-\delta\tau} d\tau \pi(dv d\Lambda) \quad (25)$$

The measure $\nu(\cap_{j \in J} A_j)$ in (25) is unchanged if both β and each y_j are multiplied by the same constant $c > 0$. By (24), the $\nu(\cup_{1 \leq i \leq n} A_i)$ is also unchanged.

Finally, by (23) and (25),

$$\begin{aligned} P[\cap_{1 \leq i \leq n} [cY_1^*(x_i, t_i) \leq y_i]] &= P\left[\cap_{1 \leq i \leq n} [Y_1^*(x_i, t_i) \leq y_i/c]\right] \\ &= P\left[\cap_{1 \leq i \leq n} [Y_c^*(x_i, t_i) \leq y_i]\right], \end{aligned}$$

proving the lemma. \square

Lemma A.2. *If $\{Y_i\}_{1 \leq i \leq n} \stackrel{\text{iid}}{\sim} \text{MSV}(\beta, \delta, \pi, \varphi)$ are independent MSV processes with maximal processes*

$$Y_i^*(x, t) := \sup_{0 \leq s \leq t} Y_i(x, s), \quad t > 0$$

then the maximum $\vee_{1 \leq i \leq n} Y_i^(x, t)$ is the maximal process $Y^*(x, t)$ for a max-stable velocity process $Y \sim \text{MSV}(n\beta, \delta, \pi, \varphi)$.*

Proof.

Each of $\{Y_i\}$ has a representation (14a) for the support points $\{\omega_j^{(i)}\}_{j \in \mathbb{N}}$ of the i th of n independent Poisson random measures $\mathcal{N}^{(i)}(d\omega) \stackrel{\text{iid}}{\sim} \text{Po}(\nu(d\omega))$ for the intensity measure $\nu(d\omega)$ of (13). The sum $\mathcal{N}^+(d\omega) := \sum_{1 \leq i \leq n} \mathcal{N}^{(i)}(d\omega) \sim \text{Po}(n\nu(d\omega))$ is also a Poisson random measure, with

intensity measure $n\nu(d\omega)$ and with support equal to the union $\{\omega_j^{(i)}\}$ of the supports of $\{\mathcal{N}^{(i)}\}$, and the max-stable velocity process $Y(x, t)$ associated with $\mathcal{N}^+(d\omega)$ by (14a) is $\vee_{1 \leq i \leq n} Y_i(x, t)$. By Theorem A.1, $Y \sim \text{MSV}(n\beta, \delta, \pi, \varphi)$. But $\vee_{1 \leq i \leq n} Y_i^*(x, t) = Y^*(x, t)$ and the Lemma follows. \square

We now prove Theorem 3.3.

Proof.

Let $\{Y_i\}_{1 \leq i \leq n} \stackrel{\text{iid}}{\sim} \text{MSV}(\beta, \delta, \pi, \varphi)$ and $Y \sim \text{MSV}(\beta, \delta, \pi, \varphi)$ be independent MSV processes with maximal processes

$$Y_i^*(x, t) := \sup_{0 \leq s \leq t} Y_i(x, s) \quad Y^*(x, t) := \sup_{0 \leq s \leq t} Y(x, s), \quad t > 0$$

By Lemma A.2, there exists a process $Y_0 \sim \text{MSV}(n\beta, \delta, \pi, \varphi)$ whose maximal process Y_0^* is the maximum $\vee_{1 \leq i \leq n} Y_i^*(x, t)$. By Lemma A.1 with $c = n$, $Y_0^* \stackrel{\mathcal{D}}{=} nY^*$, i.e., $Y^*(x, t) \stackrel{\mathcal{D}}{=} \frac{1}{n} \vee_{1 \leq i \leq n} Y_i^*(x, t)$. By (1) in Theorem 3.1, $Y^*(x, t)$ is max-stable. \square

B Proof of Theorem 3.4 and Corollaries 3.7 and 3.6

B.1 Marginal Distribution of $Y(x, t)$

Fix $x \in \mathbb{R}^d$, $t \in \mathbb{R}$, and $y > 0$. Then the event

$$[Y(x, t) \leq y] = \{\mathcal{N}(A) = 0\}$$

that $Y(x, t)$ does not exceed y is identical to the event that the Poisson random measure $\mathcal{N}(d\omega)$ assigns zero points to the set

$$A = \{\omega : \sigma < t < \sigma + \tau, u\varphi_\Lambda(x - \xi - (t - \sigma)v) > y\}$$

of particles born before time t , surviving until time t , that move from their birth point ξ at velocity v to a location $\xi_t := \xi + (t - \sigma)v$ sufficiently close to x that their intensity u will lead to exceedance of level y . We will use $\nu(\cdot)$ to denote the measure of a set with respect to the intensity measure of \mathcal{N} . The probability of the event $\mathbb{P}(\mathcal{N}(A) = 0)$ for the Poisson measure $\mathcal{N} \sim \text{Po}(\nu(d\omega))$ is

$$\begin{aligned} \mathbb{P}[Y(x, t) \leq y] &= \exp(-\nu(A)) \\ &= \exp\left(-\int_{\mathbb{R}^d \times \mathcal{P}^d \times \mathbb{R}^d} \int_{\sigma < t < \sigma + \tau} \int_{u > y/\varphi_\Lambda(x - \xi_t)} u^{-2} du \beta \delta e^{-\delta\tau} d\tau d\sigma d\xi \pi(dv d\Lambda)\right) \\ &= \exp\left(-\int_{\mathbb{R}^d \times \mathcal{P}^d \times \mathbb{R}^d} \int_{\sigma < t < \sigma + \tau} \frac{1}{y} \varphi_\Lambda(x - \xi_t) \beta \delta e^{-\delta\tau} d\tau d\sigma d\xi \pi(dv d\Lambda)\right) \\ &= \exp\left(-\int_{\mathbb{R}^d \times \mathcal{P}^d \times \mathbb{R}^d} \frac{\beta}{\delta y} \varphi_\Lambda(x - \xi - (t - \sigma)v) d\xi \pi(dv d\Lambda)\right) \\ &= \exp\left(-\frac{\beta}{\delta y}\right), \end{aligned}$$

so $Y(x, t) \sim \text{Fr}(1, \beta/\delta)$ has the unit Fréchet distribution with scale β/δ for all locations $x \in \mathbb{R}^d$ and times $t > 0$, for any probability distribution $\pi(dv d\Lambda)$.

B.2 Marginal Distribution of κ and $Y^*(x, t)$

Now suppose that $\varphi(z)$ is a monotonically decreasing function of squared Euclidean length, and denote by $\xi_s := \xi + v(s - \sigma)$ the location at time $s \in \mathbb{R}$ of the particle $\omega = (u, \xi, \sigma, \tau, \Lambda, v)$, born at location ξ at time σ . The event that the first exceedance time $\kappa(y)$ of level $y > 0$ is later than any specified $t > 0$ is the event that the Poisson random measure $\mathcal{N}(d\omega)$ assigns zero points to the Borel set

$$A := \left\{ \omega : \sup_{s \in [0, t] \cap [\sigma, \sigma + \tau]} u\varphi_\Lambda(x - \xi_s) > y \right\}, \quad (26)$$

whose probability is $\mathbb{P}[\kappa(y) > t] = \exp(-\nu(A))$. It is convenient for us to write A as the disjoint union of several simpler pieces, and then sum their measures to find $\nu(A)$. For fixed $\Lambda \in \mathcal{P}^d$ and $v \in \mathbb{R}^d$, denote by Δ the time interval (positive or negative) between birth and arrival at the closest point of approach to x (CPA), starting from ξ and traveling at velocity v , *i.e.*,

$$\begin{aligned}\Delta &:= \operatorname{argmax}_{s \in \mathbb{R}} \{\varphi_\Lambda(x - \xi - sv)\} \\ &= \operatorname{argmin}_{s \in \mathbb{R}} \{(x - \xi - sv)' \Lambda (x - \xi - sv)\} \\ &= v' \Lambda (x - \xi) / v' \Lambda v.\end{aligned}$$

Any vector $z \in \mathbb{R}^d$ can be written uniquely as the sum $z = (z^\parallel + z^\perp)$ of its projections onto the vector space spanned by the velocity vector v , and its orthogonal complement, in the inner product Λ , given by:

$$z^\parallel := (v' \Lambda z / v' \Lambda v) v \quad \quad \quad z^\perp := z - (v' \Lambda z / v' \Lambda v) v \quad (27)$$

The projection of $(x - \xi)$ onto the span of v is $(x - \xi)^\parallel = \Delta v$, and $\xi + \Delta v$ is the CPA to x .

The particle is initially *approaching* x if $v' \Lambda (x - \xi) > 0$, *i.e.*, $\Delta > 0$; otherwise it is initially *receding* from x . The supremum in (26) will be attained at time $s^* = \sigma + \Delta$, if that is in the interval $[0, t] \cap [\sigma, \sigma + \tau]$. If not, the supremum will be attained at one of the endpoints of that interval.

We write A as the disjoint union of five sets, one for each possible time

$$s^* = \operatorname{argmax} \{Y(x, s) : s \in [0, t] \cap [\sigma, \sigma + \tau]\}$$

at which $Y(x, s)$ attains its maximum in $[0, t]$: the beginning $s = 0$ or end $s = t$ of the interval, the time of the particle's birth $s = \sigma$ or death $s = \sigma + \tau$, or some intermediate point.

A_1 : $s^* \in (0, t) \cap (\sigma, \sigma + \tau)$. The particle initially approaches x (*i.e.*, $\Delta > 0$) and reaches CPA before its death or time t , whichever occurs first. The supremum $\sup_s [\varphi_\Lambda(x - \xi_s)]$ occurs at CPA time $s^* = \sigma + \Delta$, at which time $\xi_{s^*} = \xi + \Delta v$ so

$$(x - \xi_{s^*}) = x - \xi - \Delta v = (x - \xi)^\perp,$$

the projection of $(x - \xi)$ onto the orthogonal complement of v . It follows that

$$A_1 = \{\omega : u \varphi_\Lambda(x - \xi_{s^*}) > y, \quad (0 \vee \sigma) \leq (\sigma + \Delta) \leq (t \wedge (\sigma + \tau))\} \quad (28)$$

After integrating wrt $u^{-2} du$,

$$\nu(A_1) = \frac{1}{y} \int_{\mathbb{R}^d \times \mathcal{P}^d \times \mathbb{R}^d \times (-\Delta \leq \sigma \leq t - \Delta) \times (\Delta \leq \tau < \infty)} \mathbf{1}_{\{\Delta > 0\}} \beta \delta e^{-\delta \tau} \varphi_\Lambda(x - \xi_{s^*}) \, d\tau d\sigma d\xi \pi(dv \, d\Lambda)$$

Integrating wrt τ , then σ ,

$$= \frac{\beta}{y} t \int_{\mathbb{R}^d \times \mathcal{P}^d \times \mathbb{R}^d} \mathbf{1}_{\{\Delta > 0\}} e^{-\delta \Delta} \varphi_\Lambda((x - \xi)^\perp) \, d\xi \pi(dv \, d\Lambda)$$

Changing variables from ξ to (Δ, ζ) with $\Delta = v' \Lambda (x - \xi) / v' \Lambda v$ (so $\Delta v = (x - \xi)^\parallel$) and $\zeta = (x - \xi)^\perp \in v^\perp \equiv \mathbb{R}^{d-1}$, with Jacobian $|v| = \sqrt{v' \Lambda v}$, and integrating wrt Δ ,

$$= \frac{\beta}{\delta y} t \int_{\mathbb{R}^d \times \mathcal{P}^d \times \{\zeta \in v^\perp\}} \varphi_\Lambda(\zeta) \, d\zeta |v| \pi(dv \, d\Lambda). \quad (29)$$

A_2 : $s^* = t$. The particle approaches x and survives until time t but fails to reach CPA by t . The supremum $\sup_s [\varphi_\Lambda(x - \xi_s)]$ occurs at time $s^* = t$, at which time $\xi_{s^*} = \xi + (t - \sigma)v$:

$$A_2 = \{\omega : u\varphi_\Lambda(x - \xi - (t - \sigma)v) > y, \quad (0 \vee \sigma) \leq t < \sigma + (\tau \wedge \Delta)\} \quad (30)$$

After integrating wrt $u^{-2}du$, and noting that $(x - \xi_{s^*}) = (x - \xi)^\perp + (\Delta - (t - \sigma))v$ so the $d\xi$ integral extends over the half-space on which $v'\Lambda(x - \xi_{s^*}) > 0$,

$$\begin{aligned} \nu(A_2) &= \frac{1}{y} \int_{\mathbb{R}^d \times \mathcal{P}^d \times (-\infty, t] \times (t - \sigma, \infty) \times \mathbb{R}^d} \mathbf{1}_{\{\Delta > t - \sigma\}} \beta \delta e^{-\delta \tau} \varphi_\Lambda(x - \xi_{s^*}) d\xi d\tau d\sigma \pi(dv d\Lambda) \\ &= \frac{1}{2y} \int_{\mathbb{R}^d \times \mathcal{P}^d \times (-\infty, t] \times (t - \sigma, \infty)} \beta \delta e^{-\delta \tau} d\tau d\sigma \pi(dv d\Lambda) \\ &= \frac{1}{2y} \int_{(-\infty, t] \times (t - \sigma, \infty)} \beta \delta e^{-\delta \tau} d\tau d\sigma \\ &= \frac{\beta}{2\delta y}. \end{aligned} \quad (31)$$

A_3 : $s^* = \sigma + \tau$. The particle lives to time 0 and approaches x but dies before time t without reaching the CPA. The supremum $\sup_s [\varphi_\Lambda(x - \xi_s)]$ occurs at death time $s^* = \sigma + \tau$, at which time $\xi_{s^*} = \xi + \tau v$, so

$$A_3 = \{\omega : u\varphi_\Lambda(x - \xi - \tau v) > y, \quad (0 \vee \sigma) \leq \sigma + \tau \leq t \wedge (\sigma + \Delta)\} \quad (32)$$

After integrating wrt $u^{-2}du$, and noting that $(x - \xi_{s^*}) = (x - \xi)^\perp + (\Delta - \tau)v$ so the $d\xi$ integral extends over the half-space on which $v'\Lambda(x - \xi_{s^*}) > 0$,

$$\begin{aligned} \nu(A_3) &= \frac{1}{y} \int_{\mathbb{R}^d \times \mathcal{P}^d \times (0, \infty) \times (-\tau, t - \tau) \times \mathbb{R}^d} \mathbf{1}_{\{\Delta > \tau\}} \beta \delta e^{-\delta \tau} \varphi_\Lambda(x - \xi - \tau v) d\xi d\sigma d\tau \pi(dv d\Lambda) \\ &= \frac{1}{2y} \int_{\mathbb{R}^d \times \mathcal{P}^d \times (0, \infty) \times (-\tau, t - \tau)} \beta \delta e^{-\delta \tau} d\sigma d\tau \pi(dv d\Lambda) \\ &= \frac{1}{2y} \int_{(0, \infty) \times (-\tau, t - \tau)} \beta \delta e^{-\delta \tau} d\sigma d\tau \\ &= \frac{\beta}{2\delta y} \delta t. \end{aligned} \quad (33)$$

A_4 : $s^* = 0$. The particle is born before time zero, and by time zero is still alive and is receding from x (either because it receded initially, or because it passed the CPA before time zero). Because this system is invariant under time-reversal, this set has the same ν measure as the set A_2 , giving $\nu(A_4) = \beta(2\delta y)^{-1}$.

A_5 : $s^* = \sigma$. The particle was born during the interval $[0, t]$ and recedes from x . Again appealing to time-reversibility, $\nu(A_5) = \nu(A_3) = \beta(2\delta y)^{-1}$.

B.3 Summary

The ν measures of the five pieces are:

$$\begin{aligned} \nu(A_1) &= \frac{\beta}{\delta y} t \int_{\mathbb{R}^d \times \mathcal{P}^d \times \{\zeta \in v^\perp\}} \varphi_\Lambda(\zeta) d\zeta |v| \pi(dv d\Lambda) \\ \nu(A_2) &= \frac{\beta}{2\delta y} \quad \nu(A_3) = \frac{\beta}{2\delta y} \delta t \quad \nu(A_4) = \frac{\beta}{2\delta y} \quad \nu(A_5) = \frac{\beta}{2\delta y} \delta t \end{aligned}$$

whose sum is

$$\nu(A) = \frac{\beta}{\delta y} \left\{ 1 + \delta t + t \int_{\mathbb{R}^d \times \mathcal{P}^d \times \{\zeta \in v^\perp\}} \varphi_\Lambda(\zeta) d\zeta |v| \pi(dv d\Lambda) \right\}. \quad (34)$$

Thus, the probability distribution of the first time $\kappa(y)$ that $Y(x, t)$ exceeds any level y is of the form

$$\mathbb{P}[\kappa(y) > t] = \exp(-\nu(A)) = \exp\left(-\frac{\beta}{\delta y} - t \cdot \text{const}\right), \quad (35)$$

a mixture of a point-mass at zero of magnitude $1 - \exp(\beta/\delta y)$ and an exponentially-distributed random variable whose rate constant

$$\frac{\beta}{\delta y} \left\{ \delta + \int_{\mathbb{R}^d \times \mathcal{P}^d \times v^\perp} \varphi_\Lambda(\zeta) d\zeta |v| \pi(dv d\Lambda) \right\}$$

depends on the mean particle speed and kernel shape. Corollary 3.6 follows immediately since $[Y^*(x, t) < y]$ and $[\kappa(y) > t]$ are identical events.

B.4 Special Case: Gaussian Kernel

Consider the Gaussian case of $\varphi(z) = (2\pi)^{-d/2} \exp(-z'z/2)$, and fix any $\Lambda \in \mathcal{P}^d$ and $v \in \mathbb{R}^d$. The projection of $\xi \in \mathbb{R}^d$ onto the span of v (see (27)) is $\xi^\parallel = (v'\Lambda\xi/v'\Lambda v)v = \Delta v$, where $\Delta = (v'\Lambda\xi/v'\Lambda v)$, with squared Λ -length $(\xi^\parallel)'\Lambda(\xi^\parallel) = \Delta^2 v'\Lambda v$. Using (50)

$$\int_{v^\perp} \varphi_\Lambda(\zeta) d\zeta |v| = (v'\Lambda v/2\pi)^{\frac{1}{2}},$$

and $\nu(A)$ from (34) is

$$\nu(A) = \frac{\beta}{\delta y} \left\{ 1 + \delta t + t \int_{\mathbb{R}^d \times \mathcal{P}^d} (v'\Lambda v/2\pi)^{\frac{1}{2}} \pi(dv d\Lambda) \right\}. \quad (36)$$

C Proof of Corollary 3.5

It follows from Theorem 3.4 that $\mathbb{E}[|V(x_i)|^3] = c_i < \infty$ for all $x_i \in \mathcal{X}$. Let

$$V^*(x_i) = \frac{J^{-1} \sum_{j=1}^J V_j(x_i) - \mathbb{E}[V(x_i)]}{\sqrt{n^{-1} \text{var}(V(x_i))}},$$

then for an absolute constant C we have

$$\sup_t |\mathbb{P}[V^*(x_i) < t] - \Phi(t)| \leq \frac{1}{\sqrt{n}} C c_j, \quad (37)$$

where $\Phi(\cdot)$ is the standard normal distribution function. If (17) holds, then $\sup_j c_j = c < \infty$, and we can replace c_j by c in (37) for all i . The same result holds in the Wasserstein 1 metric with respect to the Euclidean distance with a different constant C . The proof for Z is essentially identical.

D Proof of Theorem 3.8

Applying the inclusion-exclusion principle and change-of-variables from ξ to $z := (\xi - v\sigma)$ to (19a) gives the result.

E Proof of Corollary 3.9

By Theorem 3.8, the joint CDF of $Y_{t_1}(x_1)$ and $Y_{t_2}(x_2)$ can be found as

$$\mathbb{P}[Y_{t_1}(x_1) \leq y_1, Y_{t_2}(x_2) \leq y_2] = \exp(-\nu(B_1 \cup B_2))$$

for the sets

$$B_i := \{\omega : \sigma < t_i < \sigma + \tau, u\varphi_\Lambda(x_i - \xi - (t_i - \sigma)v) > y_i\}$$

of particles leading to an exceedance of y_i at (x_i, t_i) for $i = 1, 2$. In Theorem 3.4, we found $\nu(B_i) = \beta/\delta y_i$. To find the required $\nu(B_1 \cup B_2) = \nu(B_1) + \nu(B_2) - \nu(B_1 \cap B_2)$ we need the measure of the intersection. Putting $\xi_{t_i} = \xi + (t_i - \sigma)v$,

$$\begin{aligned} \nu(B_1 \cap B_2) &= \int_{\mathcal{P}^d \times \mathbb{R}^d \times \mathbb{R}^d} \int_{\sigma \leq (t_1 \wedge t_2)} \\ &\quad \int_{\tau \geq (t_1 \vee t_2) - \sigma} \int_{u \geq \left(\frac{y_1}{\varphi_\Lambda(x_1 - \xi_{t_1})} \vee \frac{y_2}{\varphi_\Lambda(x_2 - \xi_{t_2})} \right)} u^{-2} du \delta e^{-\delta\tau} d\tau \beta d\sigma d\xi \pi(dv d\Lambda) \\ &= \int_{\mathcal{P}^d \times \mathbb{R}^d \times \mathbb{R}^d} \int_{\sigma \leq (t_1 \wedge t_2)} \\ &\quad \int_{\tau \geq (t_1 \vee t_2) - \sigma} \left(\frac{\varphi_\Lambda(x_1 - \xi_{t_1})}{y_1} \wedge \frac{\varphi_\Lambda(x_2 - \xi_{t_2})}{y_2} \right) \delta e^{-\delta\tau} d\tau \beta d\sigma d\xi \pi(dv d\Lambda) \\ &= \int_{\mathcal{P}^d \times \mathbb{R}^d \times \mathbb{R}^d} \int_{\sigma \leq (t_1 \wedge t_2)} \\ &\quad \left(\frac{\varphi_\Lambda(x_1 - \xi_{t_1})}{y_1} \wedge \frac{\varphi_\Lambda(x_2 - \xi_{t_2})}{y_2} \right) e^{-\delta((t_1 \vee t_2) - \sigma)} \beta d\sigma d\xi \pi(dv d\Lambda) \end{aligned}$$

Set

$$\Delta_v := (x_2 - x_1) - (t_2 - t_1)v \quad (38)$$

(which doesn't depend on σ) and change variables from ξ to $z := \xi - \frac{x_1 + x_2}{2} + v[\frac{t_1 + t_2}{2} - \sigma]$:

$$\begin{aligned} &= \int_{\mathcal{P}^d \times \mathbb{R}^d \times \mathbb{R}^d} \int_{\sigma \leq (t_1 \wedge t_2)} \left(\frac{\varphi_\Lambda(z - \Delta_v/2)}{y_1} \wedge \frac{\varphi_\Lambda(z + \Delta_v/2)}{y_2} \right) \\ &\quad e^{-\delta((t_1 \vee t_2) - \sigma)} \beta d\sigma dz \pi(dv d\Lambda) \\ &= \frac{\beta}{\delta} e^{-\delta|t_2 - t_1|} \int_{\mathcal{P}^d \times \mathbb{R}^d \times \mathbb{R}^d} \left(\frac{\varphi_\Lambda(z - \Delta_v/2)}{y_1} \wedge \frac{\varphi_\Lambda(z + \Delta_v/2)}{y_2} \right) dz \pi(dv d\Lambda), \quad (39) \end{aligned}$$

so then

$$\begin{aligned} \nu(A_1 \cup A_2) &= \frac{\beta}{\delta} \left[\frac{1}{y_1} + \frac{1}{y_2} \right] \\ &\quad - \frac{\beta}{\delta} e^{-\delta|t_2 - t_1|} \int_{\mathcal{P}^d \times \mathbb{R}^d \times \mathbb{R}^d} \left(\frac{\varphi_\Lambda(z - \Delta_v/2)}{y_1} \wedge \frac{\varphi_\Lambda(z + \Delta_v/2)}{y_2} \right) dz \pi(dv d\Lambda) \end{aligned}$$

In the Gaussian case with $\varphi(z) = (2\pi)^{-d/2} \exp(-z'z/2)$ this simplifies. Set $B_1^* := B_1 \cap B_2 \cap \{\omega : \Delta' \Lambda z < \log \frac{y_1}{y_2}\}$, the set of $\omega \in B_1 \cap B_2$ where the minimum in (39) is attained at (x_1, t_1) , and set $B_2^* = (B_1 \cap B_2) \setminus B_1^*$, the set on which it is attained at (x_2, t_2) . Then

$$\nu(B_1^*) = \frac{\beta}{\delta y_1} e^{-\delta|t_2 - t_1|} \int_{\mathcal{P}^d \times \mathbb{R}^d \times \mathbb{R}^d} \varphi_\Lambda(z - \Delta_v/2) \mathbf{1}_{\{\Delta' \Lambda z < \log \frac{y_1}{y_2}\}} dz \pi(dv d\Lambda)$$

For fixed v let $\zeta := z - (\Delta'_v \Lambda z / \Delta'_v \Lambda \Delta_v) \Delta_v$ be the orthogonal projection onto the space Δ_v^\perp perpendicular to Δ_v in the Λ norm, and change variables from z to (ζ, s) with $z = \zeta + s\Delta_v$ and Jacobian $dz = (\Delta'_v \Delta_v)^{\frac{1}{2}} d\zeta ds$, to find

$$\begin{aligned} \nu(B_1^*) &= \frac{\beta}{\delta y_1} e^{-\delta|t_2 - t_1|} \int_{\mathcal{P}^d \times \mathbb{R}^d \times \Delta_v^\perp \times \mathbb{R}} |\Lambda/2\pi|^{\frac{1}{2}} \exp(-\zeta' \Lambda \zeta/2) e^{-s^2 \Delta'_v \Lambda \Delta_v/2} \\ &\quad \mathbf{1}_{\{s < \log \frac{y_1}{y_2} / \Delta'_v \Lambda \Delta_v\}} \sqrt{\Delta'_v \Delta_v} ds d\zeta \pi(dv d\Lambda) \end{aligned}$$

$$= \frac{\beta}{\delta y_1} e^{-\delta|t_2-t_1|} \int_{\mathcal{P}^d \times \mathbb{R}^d} \Phi\left(\frac{\log \frac{y_1}{y_2}}{S_\Lambda(v)} - \frac{1}{2} S_\Lambda(v)\right) \pi(dv d\Lambda)$$

where $S_\Lambda(v) := \sqrt{\Delta'_v \Lambda \Delta_v}$. Similarly,

$$\begin{aligned} \nu(B_2^*) &= \frac{\beta}{\delta y_2} e^{-\delta|t_2-t_1|} \int_{\mathcal{P}^d \times \mathbb{R}^d} \Phi\left(\frac{\log \frac{y_2}{y_1}}{S_\Lambda(v)} - \frac{1}{2} S_\Lambda(v)\right) \pi(dv d\Lambda), \quad \text{so} \\ \nu(B_1 \cap B_2) &= \nu(B_1^*) + \nu(B_2^*) = \frac{\beta}{\delta} e^{-\delta|t_2-t_1|} \int_{\mathcal{P}^d \times \mathbb{R}^d} \left\{ \frac{1}{y_1} \Phi\left(\frac{\log \frac{y_1}{y_2}}{S_\Lambda(v)} - \frac{1}{2} S_\Lambda(v)\right) + \right. \\ &\quad \left. + \frac{1}{y_2} \Phi\left(\frac{\log \frac{y_2}{y_1}}{S_\Lambda(v)} - \frac{1}{2} S_\Lambda(v)\right) \right\} \pi(dv d\Lambda) \end{aligned}$$

and

$$\begin{aligned} \nu(B_1 \cup B_2) &= \frac{\beta}{\delta} \left(\frac{1}{y_1} + \frac{1}{y_2} \right) - \nu(B_1 \cap B_2) \\ &= \frac{\beta}{\delta} \left(1 - e^{-\delta|t_2-t_1|} \right) \left(\frac{1}{y_1} + \frac{1}{y_2} \right) \\ &\quad + \frac{\beta}{\delta} e^{-\delta|t_2-t_1|} \int_{\mathcal{P}^d \times \mathbb{R}^d} \left\{ \frac{1}{y_1} \Phi\left(\frac{1}{2} S_\Lambda(v) - \frac{\log \frac{y_1}{y_2}}{S_\Lambda(v)}\right) + \right. \\ &\quad \left. + \frac{1}{y_2} \Phi\left(\frac{1}{2} S_\Lambda(v) - \frac{\log \frac{y_2}{y_1}}{S_\Lambda(v)}\right) \right\} \pi(dv d\Lambda). \end{aligned} \tag{40}$$

F Proof of Theorem 3.10

In this section we compute a lower bound for the probability of two exceedances $Y(x_j, s_j) > y_j$, $j = 1, 2$ of levels $\{y_j\} \subset \mathbb{R}_+$ at locations $\{x_j\} \subset \mathbb{R}^d$ within the interval $\{s_j\} \subset [0, t]$ for $t > 0$. Some calculations used in the sequel are found in Section H.

F.1 General case

We consider the case in which CPA is attained at both points during the interval $[0, t]$ for the general max-stable velocity process. For $j = 1, 2$ set:

$$\begin{aligned} \Delta_j &:= \operatorname{argmax}_{s \in \mathbb{R}} \{ \varphi_\Lambda(x_j - \xi - sv) \} = v' \Lambda(x_j - \xi) / v' \Lambda v \\ s_j^* &:= \operatorname{argmax}_{s \in [0, t] \cap [\sigma, \sigma + \tau]} \{ \varphi_\Lambda(x_j - \xi - (s - \sigma)v) \} \\ u_j^* &:= \frac{y_j}{\varphi_\Lambda(x_j - \xi_{s_j^*})}. \end{aligned}$$

To achieve exceedance and CPA at both locations a particle must satisfy

$$u > u_1^* \vee u_2^* \quad s_j^* = \sigma + \Delta_j \in [0, t] \cap [\sigma, \sigma + \tau], \quad j = 1, 2. \tag{41}$$

Write the set $A \subset \Omega$ of particles that satisfy these conditions as the union of four sets

$$A_{ij} := \{ \omega \in \Omega : \Delta_i = (\Delta_1 \wedge \Delta_2), \quad u_j^* = (u_1^* \vee u_2^*) \} \quad i, j = 1, 2 \tag{42}$$

characterized by which CPA occurs first and which exceedance requires the larger mass u . For example,

$$A_{11} = \{ \omega \in \Omega : u > u_1^* > u_2^*, (0 \vee \sigma) < \sigma + \Delta_1 < \sigma + \Delta_2 < t \wedge (\sigma + \tau) \}$$

consists of the particles that initially approach both x_1 and x_2 and reach CPA for both before their death. Both suprema $\sup_s [\varphi_\Lambda(x - \xi_s)]$ occur at the CPA times $s_j^* = \sigma + \Delta_j$, at CPA locations $\xi_{s_j^*} = \xi + \Delta_j v$, so

$$(x_j - \xi_{s_j^*}) = (x_j - \xi - \Delta_j v) = (x_j - \xi)^\perp$$

is the projection of $(x_j - \xi)$ onto the orthogonal complement of v for $j = 1, 2$. After integrating wrt $u^{-2} du$, we have

$$\nu(A_{11}) = \frac{1}{y_1} \int_{\times_{\substack{\mathbb{R}^d \times \mathcal{P}^d \times \mathbb{R}^d \\ \times_{\substack{(-\Delta_1 < \sigma < t - \Delta_2) \\ \times (\Delta_2 < \tau < \infty)}}}} \mathbf{1}_{\{0 < \Delta_1 < \Delta_2\}} \mathbf{1}_{\{u_1^* > u_2^*\}} \beta \delta e^{-\delta \tau} \varphi_\Lambda((x_1 - \xi)^\perp) d\tau d\sigma d\xi \pi(dv d\Lambda)$$

Integrating with respect to τ then σ ,

$$= \frac{\beta}{y_1} \int_{\mathbb{R}^d \times \mathcal{P}^d \times \mathbb{R}^d} (t - (\Delta_2 - \Delta_1)) e^{-\delta \Delta_2} \varphi_\Lambda((x_1 - \xi)^\perp) \times \mathbf{1}_{\{0 < \Delta_1 < \Delta_2\}} \mathbf{1}_{\{\Delta_2 - \Delta_1 \leq t\}} \mathbf{1}_{\{u_1^* > u_2^*\}} d\xi \pi(dv d\Lambda). \quad (43)$$

Change variables from $\xi \in \mathbb{R}^d$ to $(\zeta, \gamma) \in v^\perp \times v^\parallel$ with

$$\zeta := \left(\frac{x_1 + x_2}{2} - \xi \right)^\perp, \quad \gamma := \left(\frac{x_1 + x_2}{2} - \xi \right)^\parallel$$

and introduce the quantity

$$\Delta_{12} := (\Delta_2 - \Delta_1) = v' \Lambda (x_2 - x_1) / v' \Lambda v,$$

noting that it doesn't depend on ξ . With this we can write

$$\Delta_1 = -\frac{1}{2} \Delta_{12} + v' \Lambda \gamma / v' \Lambda v \quad \Delta_2 = +\frac{1}{2} \Delta_{12} + v' \Lambda \gamma / v' \Lambda v.$$

Introduce $\mu := \frac{1}{2}(x_2 - x_1)^\perp$ and note that

$$\varphi_\Lambda(x_1 - \xi_{s_j^*}) = \varphi_\Lambda((x_1 - \xi)^\perp) = \varphi_\Lambda(\zeta - \mu) \quad (44a)$$

$$\varphi_\Lambda(x_2 - \xi_{s_j^*}) = \varphi_\Lambda((x_2 - \xi)^\perp) = \varphi_\Lambda(\zeta + \mu) \quad (44b)$$

The limits imposed by the indicator functions in (43) are:

$$\begin{aligned} 0 \leq \Delta_2 - \Delta_1 \leq t &\Leftrightarrow 0 \leq v' \Lambda (x_2 - x_1) \leq t v' \Lambda v \\ 0 \leq \Delta_1 &\Leftrightarrow \Delta_{12} v' \Lambda v \leq 2 v' \Lambda \gamma \\ u_2^* \leq u_1^* &\Leftrightarrow \varphi_\Lambda(\zeta - \mu) / \varphi_\Lambda(\zeta + \mu) \leq y_1 / y_2 \end{aligned}$$

Rewriting (43) with this variable change, then integrating wrt γ , gives

$$\begin{aligned} \nu(A_{11}) &= \frac{\beta}{y_1} \int_{\mathbb{R}^d \times \mathcal{P}^d \times v^\perp \times v^\parallel} (t - \Delta_{12}) e^{-\delta \Delta_{12}/2 - \delta v' \Lambda \gamma / v' \Lambda v} \varphi_\Lambda(\zeta - \mu) \times \\ &\quad \mathbf{1}_{\{0 \leq v' \Lambda (x_2 - x_1) \leq t v' \Lambda v\}} \mathbf{1}_{\{\Delta_{12} v' \Lambda v \leq 2 v' \Lambda \gamma\}} \mathbf{1}_{\{\varphi_\Lambda(\zeta - \mu) / \varphi_\Lambda(\zeta + \mu) \leq y_1 / y_2\}} d\gamma d\zeta \pi(dv d\Lambda) \\ &= \frac{\beta}{\delta y_1} \int_{\mathbb{R}^d \times \mathcal{P}^d} (t - \Delta_{12}) e^{-\delta \Delta_{12}} \mathbf{1}_{\{0 \leq v' \Lambda (x_2 - x_1) \leq t v' \Lambda v\}} \times \\ &\quad \left\{ \int_{\zeta \in v^\perp: \frac{\varphi_\Lambda(\zeta - \mu)}{\varphi_\Lambda(\zeta + \mu)} \leq \frac{y_1}{y_2}} \varphi_\Lambda(\zeta - \mu) d\zeta \right\} |v| \pi(dv d\Lambda). \end{aligned} \quad (45)$$

Now, we find the measure of the other three sets. First

$$A_{21} = \{\omega \in \Omega : u > u_2^* > u_1^*, (0 \vee \sigma) < \sigma + \Delta_1 < \sigma + \Delta_2 < t \wedge (\sigma + \tau)\},$$

giving

$$\begin{aligned} \nu(A_{21}) = & \frac{\beta}{\delta y_2} \int_{\mathbb{R}^d \times \mathcal{P}^d} (t - \Delta_{12}) e^{-\delta \Delta_{12}} \mathbf{1}_{\{0 \leq v' \Lambda(x_2 - x_1) \leq t v' \Lambda v\}} \times \\ & \left\{ \int_{\zeta \in v^\perp: \frac{\varphi_\Lambda(\zeta - \mu)}{\varphi_\Lambda(\zeta + \mu)} \geq \frac{y_1}{y_2}} \varphi_\Lambda(\zeta + \mu) d\zeta \right\} |v| \pi(dv d\Lambda). \end{aligned} \quad (46)$$

Finally, it is clear that with

$$\begin{aligned} A_{12} &= \{\omega \in \Omega : u > u_1^* > u_2^*, (0 \vee \sigma) < \sigma + \Delta_2 < \sigma + \Delta_1 < t \wedge (\sigma + \tau)\} \\ A_{22} &= \{\omega \in \Omega : u > u_2^* > u_1^*, (0 \vee \sigma) < \sigma + \Delta_2 < \sigma + \Delta_1 < t \wedge (\sigma + \tau)\} \end{aligned}$$

we have

$$\begin{aligned} \nu(A_{12}) &= \frac{\beta}{\delta y_1} \int_{\mathbb{R}^d \times \mathcal{P}^d} (t + \Delta_{12}) e^{\delta \Delta_{12}} \mathbf{1}_{\{0 \leq -v' \Lambda(x_2 - x_1) \leq t v' \Lambda v\}} \times \\ & \quad \left\{ \int_{\zeta \in v^\perp: \frac{\varphi_\Lambda(\zeta - \mu)}{\varphi_\Lambda(\zeta + \mu)} \leq \frac{y_1}{y_2}} \varphi_\Lambda(\zeta - \mu) d\zeta \right\} |v| \pi(dv d\Lambda). \\ \nu(A_{22}) &= \frac{\beta}{\delta y_2} \int_{\mathbb{R}^d \times \mathcal{P}^d} (t + \Delta_{12}) e^{\delta \Delta_{12}} \mathbf{1}_{\{0 \leq -v' \Lambda(x_2 - x_1) \leq t v' \Lambda v\}} \times \\ & \quad \left\{ \int_{\zeta \in v^\perp: \frac{\varphi_\Lambda(\zeta - \mu)}{\varphi_\Lambda(\zeta + \mu)} \geq \frac{y_1}{y_2}} \varphi_\Lambda(\zeta + \mu) d\zeta \right\} |v| \pi(dv d\Lambda). \end{aligned}$$

F.2 Gaussian case

Now take $\varphi(z) = (2\pi)^{-d/2} \exp(-z'z/2)$ and fix $v, \Lambda \in \mathbb{R}^d \times \mathcal{P}^d$. The set of $\zeta \in v^\perp$ over which the bracketed integral in (45) is taken can be written as:

$$\begin{aligned} \varphi_\Lambda(\zeta - \mu) &\leq \frac{y_1}{y_2} \varphi_\Lambda(\zeta + \mu) \\ -\frac{1}{2}(\zeta - \mu)' \Lambda (\zeta - \mu) &\leq \log \frac{y_1}{y_2} - \frac{1}{2}(\zeta + \mu)' \Lambda (\zeta + \mu) \\ \mu' \Lambda \zeta &\leq \frac{1}{2} \log \frac{y_1}{y_2} \end{aligned}$$

Writing $\zeta \in v^\perp$ as the sum $\zeta = \zeta_\perp + \zeta_\parallel$ of components orthogonal and parallel to $(x_2 - x_1)^\perp$ (in the Λ metric), by (53),

$$\nu(A_{11}) = \frac{\beta}{y_1} \int_{\substack{\mathbb{R}^d \times \mathcal{P}^d \\ 0 \leq \Delta_{12} \leq t}} (t - \Delta_{12}) e^{-\delta \Delta_{12}} \sqrt{v' \Lambda v / 2\pi} \Phi\left(-\frac{S_\Lambda^\perp(v)}{2} + \frac{\log(y_1/y_2)}{S_\Lambda^\perp(v)}\right) \pi(dv d\Lambda).$$

with $S_\Lambda^\perp(v) := \{(x_2 - x_1)' \Lambda (x_2 - x_1)^\perp\}^{1/2}$. The other three sets have measure

$$\begin{aligned} \nu(A_{21}) &= \frac{\beta}{y_2} \int_{\substack{\mathbb{R}^d \times \mathcal{P}^d \\ 0 \leq \Delta_{12} \leq t}} (t - \Delta_{12}) e^{-\delta \Delta_{12}} \sqrt{v' \Lambda v / 2\pi} \Phi\left(-\frac{S_\Lambda^\perp(v)}{2} - \frac{\log(y_1/y_2)}{S_\Lambda^\perp(v)}\right) \pi(dv d\Lambda). \\ \nu(A_{12}) &= \frac{\beta}{y_1} \int_{\substack{\mathbb{R}^d \times \mathcal{P}^d \\ 0 \leq -\Delta_{12} \leq t}} (t + \Delta_{12}) e^{\delta \Delta_{12}} \sqrt{v' \Lambda v / 2\pi} \Phi\left(-\frac{S_\Lambda^\perp(v)}{2} + \frac{\log(y_1/y_2)}{S_\Lambda^\perp(v)}\right) \pi(dv d\Lambda). \\ \nu(A_{22}) &= \frac{\beta}{y_2} \int_{\substack{\mathbb{R}^d \times \mathcal{P}^d \\ 0 \leq -\Delta_{12} \leq t}} (t + \Delta_{12}) e^{\delta \Delta_{12}} \sqrt{v' \Lambda v / 2\pi} \Phi\left(-\frac{S_\Lambda^\perp(v)}{2} - \frac{\log(y_1/y_2)}{S_\Lambda^\perp(v)}\right) \pi(dv d\Lambda). \end{aligned}$$

Recognizing a simple change of variables, we have

$$\nu(A) = \frac{\beta}{\sqrt{2\pi}} \int_{\substack{\mathbb{R}^d \times \mathcal{P}^d \\ \cap \{-t \leq \Delta_{12} \leq t\}}} (t - \Delta_{12}) e^{-\delta \Delta_{12}} \left\{ \frac{1}{y_1} \Phi\left(-\frac{S_\Lambda^\perp(v)}{2} + \frac{\log(y_1/y_2)}{S_\Lambda^\perp(v)}\right) \right.$$

$$+ \frac{1}{y_2} \Phi \left(-\frac{S_\Lambda^\perp(v)}{2} - \frac{\log(y_1/y_2)}{S_\Lambda^\perp(v)} \right) \Big\} \sqrt{v' \Lambda v} \pi(dv d\Lambda)$$

where $A = A_{11} \cup A_{12} \cup A_{21} \cup A_{22}$. So

$$\begin{aligned} \mathbb{P}[|\kappa_2 - \kappa_1| > t] &\leq 1 - \mathbb{P}[\kappa_1 \vee \kappa_2 \leq t] \\ &\leq 1 - \mathbb{P}[\text{CPA Exceedances at } x_1, x_2 \text{ in } [0, t]] \\ &\leq \exp \{ -\nu(A) \}, \end{aligned}$$

so the probability $\mathbb{P}[|\kappa_2 - \kappa_1| > t] \rightarrow 0$ as $\mathbb{E}_\pi \left[\sqrt{v' \Lambda v} \Phi \left(-\sqrt{(x_2 - x_1)' \Lambda (x_2 - x_1)^\perp} \right) \right] \rightarrow \infty$.

G Proof of Corollary 3.11

Any point $\omega \in A$ for the set A in Theorem 3.10 is in either

$$B_1 := \{\omega : Z(x_1, x_2) < t\}, \text{ or } B_2 := \{\omega : Z(x_2, x_1) < t\}.$$

Letting $A_1 = A \cap B_1$, $A_2 = A \cap B_2$, we have $A = A_1 \cup A_2$, and therefore

$$\nu(A) \leq \nu(A_1) + \nu(A_2),$$

so either $\nu(A_1) > \frac{1}{2}\nu(A)$ or $\nu(A_2) > \frac{1}{2}\nu(A)$.

H Some Important Integrals

As before, fix $v, x_1, x_2, \xi \in \mathbb{R}^d$ and $\Lambda \in \mathcal{P}^d$, and set

$$\Delta_j := v' \Lambda (x_i - \xi) \quad \Delta_{12} := (\Delta_2 - \Delta_1) = v' \Lambda (x_2 - x_1) \quad \mu := \frac{1}{2}(x_2 - x_1)^\perp$$

where, as before, for any $z \in \mathbb{R}^d$ we denote the projections of z parallel and orthogonal to v in the Λ metric by

$$z^\parallel := (v' \Lambda z / v' \Lambda v) v \quad z^\perp = z - z^\parallel$$

and the value of the kernel function at z by

$$\varphi_\Lambda(z) := |\Lambda/2\pi|^{\frac{1}{2}} \exp(-z' \Lambda z/2)$$

Then

$$\begin{aligned} \int_{\mathbb{R}^d} \exp(-\tfrac{1}{2} \xi' \Lambda \xi) d\xi &= |\Lambda/2\pi|^{\frac{1}{2}} \\ \int_{v^\parallel} \exp(-\tfrac{1}{2} \gamma' \Lambda \gamma) d\gamma &= \int_{\mathbb{R}} \exp(-s^2 v' \Lambda v/2) |v| ds \end{aligned} \tag{47}$$

with the CoV $\gamma = sv$ with Jacobian $d\gamma = \sqrt{v' \Lambda v} ds$

$$= (v' \Lambda v/2\pi)^{-\frac{1}{2}} |v| \tag{48}$$

$$\begin{aligned} \int_{v^\perp} \exp(-\tfrac{1}{2} \zeta' \Lambda \zeta) d\zeta &= \text{the ratio of (47)/(48)} \\ &= |\Lambda/2\pi|^{\frac{1}{2}} (v' \Lambda v/2\pi)^{\frac{1}{2}} / |v|, \text{ so} \end{aligned} \tag{49}$$

$$\begin{aligned} \int_{v^\perp} \varphi_\Lambda(\zeta) d\zeta &= (v' \Lambda v/2\pi)^{\frac{1}{2}} / |v|. \\ \int_{\mu^\parallel} \exp(-\tfrac{1}{2} w' \Lambda w) dw &= \int_{\mathbb{R}} \exp(-s^2 \mu' \Lambda \mu/2) |\mu| ds \end{aligned} \tag{50}$$

Table 2: Key indicating identity of currencies in Figure 6.

col./row #	symbol	name	col./row #	symbol	name
1	AUD	Australian Dollar	7	NLG	Dutch Guilder
2	BEF	Belgian Franc	8	NZD	New Zealand Dollar
3	CAD	Canadian Dollar	9	ESP	Spanish Peseta
4	FRF	French Franc	10	SEK	Swedish Kroner
5	DEM	German Deutschmark	11	CHF	Swiss Franc
6	JPY	Japanese Yen	12	GBP	British Pound

Table 3: Key indicating identity of stocks in the images in Figure ??

col./row #	symbol	name	col./row #	symbol	name
1	axp	American Express	16	mcd	McDonald's
2	ba	Boeing	17	mmm	3M
3	cat	Caterpillar	18	mrk	Merck
4	csc	Cisco Systems	19	msft	Microsoft
5	cvx	Chevron	20	nke	Nike
6	dd	DuPont	21	pfe	Pfizer
7	dis	Disney	22	pg	Proctor & Gamble
8	ge	General Electric	23	t	AT&T
9	gs	Goldman Sachs	24	trv	Travelers
10	hd	Home Depot	25	unh	United Healthcare
11	ibm	IBM	26	utx	United Technologies
12	intc	Intel	27	v	Visa
13	jnj	Johnson & Johnson	28	vz	Verizon
14	jpm	J.P. Morgan Chase	29	wmt	Wal-Mart
15	ko	Coca-Cola	30	xom	Exxon-Mobil

$$= (\mu' \Lambda \mu / 2\pi)^{-\frac{1}{2}} |\mu| \quad (51)$$

$$\begin{aligned} \int_{\{v, \mu\}^\perp} \exp\left(-\frac{1}{2} q' \Lambda q\right) dq &= \text{the ratio of (49)/(51)} \\ &= |\Lambda / 2\pi|^{\frac{1}{2}} (v' \Lambda v \mu' \Lambda \mu)^{\frac{1}{2}} / 2\pi |v| |\mu|, \text{ so} \\ \int_{\{v, \mu\}^\perp} \varphi_\Lambda(\zeta) d\zeta &= (v' \Lambda v \mu' \Lambda \mu)^{\frac{1}{2}} / 2\pi |v| |\mu|. \end{aligned} \quad (52)$$

If the integral in (51) extends only over those $\zeta \in \mu^\parallel$ with $\mu' \Lambda \zeta \leq \frac{1}{2} \log(y_1/y_2)$, its value is reduced by a factor of $\Phi\left(\frac{\log(y_1/y_2) - 2\mu' \Lambda \mu}{2\sqrt{\mu' \Lambda \mu}}\right)$, leading to

$$\int_{v^\perp} \varphi_\Lambda(\zeta - \mu) \mathbf{1}_{\{\mu' \Lambda \zeta \geq \frac{1}{2} \log(y_1/y_2)\}} d\zeta = \Phi\left(\frac{\frac{1}{2} \log \frac{y_1}{y_2} - \mu' \Lambda \mu}{\sqrt{\mu' \Lambda \mu}}\right) \left(\frac{v' \Lambda v}{2\pi v' v}\right)^{\frac{1}{2}}. \quad (53)$$

I Additional figures

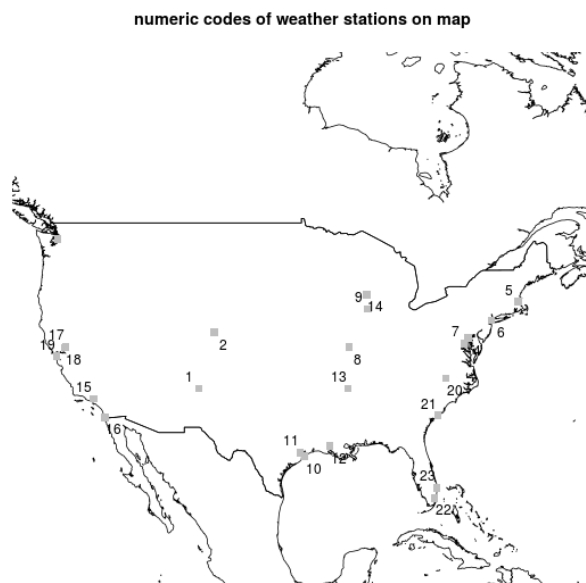


Figure 9: Map with numbers labeling locations of weather stations; the numbers correspond to the order in which the stations appear in the colormap images in Figure 5.

References

- [1] Balkema, G. and Embrechts, P. (2007). *High risk scenarios and extremes: a geometric approach*. European Mathematical Society.
- [2] Ballani, F. and Schlather, M. (2011). A construction principle for multivariate extreme value distributions. *Biometrika*, 98(3):633–645.
- [3] Beirlant, J., Goegebeur, Y., Segers, J., and Teugels, J. (2006). *Statistics of extremes: theory and applications*. John Wiley & Sons.
- [4] Buishand, T. A., de Haan, L., and Zhou, C. (2008). On spatial extremes: with application to a rainfall problem. *The Annals of Applied Statistics*, 2(2):624–642.
- [5] Coles, S. (2001). *An introduction to statistical modeling of extreme values*. Springer.
- [6] Coles, S. G. and Tawn, J. A. (1991). Modelling extreme multivariate events. *Journal of the Royal Statistical Society. Series B (Methodological)*, 53(2):377–392.
- [7] Coles, S. G. and Tawn, J. A. (1996). Modelling extremes of the areal rainfall process. *Journal of the Royal Statistical Society. Series B (Methodological)*, 58(2):329–347.
- [8] Coles, S. G. and Walshaw, D. (1994). Directional modelling of extreme wind speeds. *Journal of the Royal Statistical Society, Series C (Applied Statistics)*, 43(1):139–157.
- [9] Das, B. and Resnick, S. I. (2011). Conditioning on an extreme component: Model consistency with regular variation on cones. *Bernoulli*, 17(1):226–252.
- [10] Davis, R. A., Klüppelberg, C., and Steinkohl, C. (2013). Max-stable processes for modeling extremes observed in space and time. *Journal of the Korean Statistical Society*, 42(3):399–414.
- [11] Davison, A. C. and Smith, R. L. (1990). Models for exceedances over high thresholds. *Journal of the Royal Statistical Society. Series B (Methodological)*, 52(3):393–442.

- [12] de Haan, L. (1984). A spectral representation for max-stable processes. *The Annals of Probability*, 12(4):1194–1204.
- [13] de Haan, L. and Ferreira, A. (2006). *Extreme value theory: an introduction*. Springer.
- [14] Dzirasa, K., Phillips, H. W., Sotnikova, T. D., Salahpour, A., Kumar, S., Gainetdinov, R. R., Caron, M. G., and Nicolelis, M. A. L. (2010). Noradrenergic control of cortico-striato-thalamic and mesolimbic cross-structural synchrony. *The Journal of Neuroscience*, 30(18):6387–6397.
- [15] Embrechts, P., Koch, E., and Robert, C. (2016). Space–time max-stable models with spectral separability. *Advances in Applied Probability*, 48(A):77–97.
- [16] Gretton, A., Borgwardt, K. M., Rasch, M., Schölkopf, B., and Smola, A. J. (2006). A kernel method for the two-sample-problem. In *Advances in neural information processing systems*, pages 513–520.
- [17] Gretton, A., Borgwardt, K. M., Rasch, M. J., Schölkopf, B., and Smola, A. (2012). A kernel two-sample test. *The Journal of Machine Learning Research*, 13(1):723–773.
- [18] Gumbel, E. J. (1960a). Bivariate exponential distributions. *Journal of the American Statistical Association*, 55(292):698–707.
- [19] Gumbel, E. J. (1960b). Distributions des valeurs extrêmes en plusieurs dimensions. *Publ. Inst. Statist. Univ. Paris*, 9:171–173.
- [20] Harrison, J. and West, M. (1999). *Bayesian Forecasting & Dynamic Models*. Springer.
- [21] Heffernan, J. E. and Resnick, S. I. (2007). Limit laws for random vectors with an extreme component. *The Annals of Applied Probability*, 17(2):537–571.
- [22] Heffernan, J. E. and Tawn, J. A. (2004). A conditional approach for multivariate extreme values (with discussion). *Journal of the Royal Statistical Society: Series B (Statistical Methodology)*, 66(3):497–546.
- [23] Huser, R. and Davison, A. C. (2014). Space–time modelling of extreme events. *Journal of the Royal Statistical Society: Series B (Statistical Methodology)*, 76(2):439–461.
- [24] Hüsler, J. and Reiss, R.-D. (1989). Maxima of normal random vectors: between independence and complete dependence. *Statistics & Probability Letters*, 7(4):283–286.
- [25] Minsker, S., Srivastava, S., Lin, L., and Dunson, D. B. (2017). Robust and scalable Bayes via a median of subset posterior measures. *The Journal of Machine Learning Research*, 18(1):4488–4527.
- [26] Peres, Y. and Sousi, P. (2015). Mixing times are hitting times of large sets. *Journal of Theoretical Probability*, 28(2):488–519.
- [27] Pickands, J. (1981). Multivariate extreme value distributions. In *Proceedings 43rd Session International Statistical Institute*, volume 2, pages 859–878.
- [28] Prado, R. and West, M. (2010). *Time series: modeling, computation, and inference*. CRC Press.
- [29] Resnick, S. I. and Roy, R. (1991). Random USC functions, max-stable processes and continuous choice. *The Annals of Applied Probability*, 1(2):267–292.
- [30] Rootzén, H. and Tajvidi, N. (2006). Multivariate generalized Pareto distributions. *Bernoulli*, 12(5):917–930.
- [31] Schlather, M. (2002). Models for stationary max-stable random fields. *Extremes*, 5(1):33–44.
- [32] Schlather, M. and Tawn, J. A. (2003). A dependence measure for multivariate and spatial extreme values: Properties and inference. *Biometrika*, 90(1):139–156.

- [33] Smith, R. L. (1984). Threshold methods for sample extremes. In *Statistical extremes and applications*, pages 621–638. Springer.
- [34] Smith, R. L. (1990). Max-stable processes and spatial extremes. *Unpublished manuscript, University of Surrey*.
- [35] Smola, A., Gretton, A., Song, L., and Schölkopf (2007). Hilbert space embeddings for distributions. In *Proceedings of the 18th International Conference on Algorithmic Learning*, pages 18–31. Springer.
- [36] Song, L., Huang, J., Smola, A., and Fukumizu, K. (2009). Hilbert space embeddings of conditional distributions with applications to dynamical systems. In *Proceedings of the 26th Annual International Conference on Machine Learning*, pages 961–968. ACM.
- [37] Sriperumbudur, B. K., Gretton, A., Fukumizu, K., Schölkopf, B., and Lanckriet, G. R. G. (2010). Hilbert space embeddings and metrics on probability measures. *The Journal of Machine Learning Research*, 11:1517–1561.
- [38] Tawn, J. A. (1988). Bivariate extreme value theory: models and estimation. *Biometrika*, 75(3):397–415.
- [39] Tawn, J. A. (1990). Modelling multivariate extreme value distributions. *Biometrika*, 77(2):245–253.
- [40] Welch, B. L. (1947). The generalization of student’s problem when several different population variances are involved. *Biometrika*, 34(1/2):28–35.